FGF and retinoic acid activity gradients control the timing of neural crest cell emigration in the trunk

Patricia L. Martínez-Morales,[1] Ruth Diez del Corral,[1] Isabel Olivera-Martínez,[2] Alejandra C. Quiroga,[1] Raman M. Das,[2] Julio A. Barbas,[1] Kate G. Storey,[2] and Aixa V. Morales[1]

[1]Instituto Cajal, Consejo Superior de Investigaciones Científicas, 28002 Madrid, Spain
[2]College of Life Sciences, University of Dundee, Dundee DD1 5EH, Scotland, UK

Coordination between functionally related adjacent tissues is essential during development. For example, formation of trunk neural crest cells (NCCs) is highly influenced by the adjacent mesoderm, but the molecular mechanism involved is not well understood. As part of this mechanism, fibroblast growth factor (FGF) and retinoic acid (RA) mesodermal gradients control the onset of neurogenesis in the extending neural tube. In this paper, using gain- and loss-of-function experiments, we show that caudal FGF signaling prevents premature specification of NCCs and, consequently, premature epithelial–mesenchymal transition (EMT) to allow cell emigration. In contrast, rostrally generated RA promotes EMT of NCCs at somitic levels. Furthermore, we show that FGF and RA signaling control EMT in part through the modulation of elements of the bone morphogenetic protein and Wnt signaling pathways. These data establish a clear role for opposition of FGF and RA signaling in control of the timing of NCC EMT and emigration and, consequently, coordination of the development of the central and peripheral nervous system during vertebrate trunk elongation.

Introduction

The neural crest is formed by a transient population of multipotent cells that arises from the dorsal neural tube. Once specified, neural crest cells (NCCs) undergo a process of epithelial–mesenchymal transition (EMT) that confers the ability to delaminate and migrate away from the dorsal neural tube. The NCCs migrate along characteristic pathways to differentiate into a wide variety of derivatives according to their rostro-caudal (R-C) position in the neural tube and to the order of emigration (Krispin et al., 2010). NCC derivatives include craniofacial skeleton, sensory neurons and glia, sympathetic neurons, and melanocytes, among others (Le Douarin and Kalcheim, 1999).

The process of neural crest formation implies the orchestration of a complex gene regulatory network (Morales et al., 2005; Sauka-Spengler and Bronner-Fraser, 2008). It involves signaling pathways and transcription factors that are responsible for the sequence of early induction of the NCC during gastrulation (Wnt, bone morphogenetic proteins [BMPs], FGF, and retinoic acid [RA]; Liem et al., 1995; Saint-Jeannet et al., 1997; Villanueva et al., 2002; Monsoro-Burq et al., 2003), the specification of the neural plate border (Msx1/2, Pax3, Pax7, and Zic1/3; Liem et al., 1995; Nakata et al., 1997; Brewster et al., 1998), the expression of bona fide NCC transcription factors (AP2, Snail2, FoxD3, Sox5, Sox9, and Sox10; Nieto et al., 1994; Dottori et al., 2001; Kos et al., 2001; Paratore et al., 2001; Cheung and Briscoe, 2003; Barrallo-Gimeno et al., 2004; Perez-Alcala et al., 2004), and the regulation of numerous downstream effectors involved in cell adhesion and cell cycle control, among others (Sauka-Spengler and Bronner-Fraser, 2008).

Several neural crest specifier genes are coexpressed with neural plate border specifiers at early stages during gastrulation, suggesting possible early regulatory relationships (Khudyakov and Bronner-Fraser, 2009). However, this early population of neural crest progenitors mostly represents the cephalic NCCs, whereas the trunk neural crest progenitors will progressively be specified as the trunk neural tube elongates (Le Douarin and

P.L. Martínez-Morales and R. Diez del Corral contributed equally to this paper.

Correspondence to Aixa V. Morales: aixamorales@cajal.csic.es

I. Olivera-Martínez's present address is Centre National de la Recherche Scientifique, Université Pierre et Marie Curie, 75252 Paris, Cedex 05, France.

Abbreviations used in this paper: BMP, bone morphogenetic protein; EMT, epithelial–mesenchymal transition; ERK, extracellular signal-regulated kinase; FGFR, FGF receptor; GPI, glycosylphosphatidylinositol; HH, Hamburger and Hamilton; IRES, internal ribosome entry site; NCC, neural crest cell; PI3K, phosphatidylinositol 3-kinase; PSM, presomitic mesoderm; RA, retinoic acid; RAR, RA receptor; RARE, RA response element; R-C, rostro-caudal; VAD, vitamin A deficient; VEGFR, VEGF receptor.

The Rockefeller University Press $30.00
J. Cell Biol. Vol. 194 No. 3 489–503
www.jcb.org/cgi/doi/10.1083/jcb.201011077

Kalcheim, 1999). In that sense, the role of BMP, FGF, and Wnt signaling in the early NCC induction has been derived from work in *Xenopus laevis* at cephalic NCC territory. Thus, the signal-promoting trunk neural crest specification has not been fully elucidated.

The development of trunk NCCs is highly coordinated with the development of functionally related adjacent territories. In particular, flanking the neural tube, the paraxial or presomitic mesoderm (PSM) gets progressively segmented into smaller units, somites, and this metamerization imposes a segmented organization to the trunk NCCs. First, opposite the PSM, NCCs are confined to the dorsal neural tube, whereas NCC emigration begins facing epithelial somites (Teillet et al., 1987; Sela-Donenfeld and Kalcheim, 1999). Moreover, the first indication of peripheral nervous system segmentation is the patterned ventral migration of NCCs through the anterior part of each somitic sclerotome (Tosney, 1978; Rickmann et al., 1985; Bronner-Fraser, 1986; Loring and Erickson, 1987).

There is little knowledge about the integration of signals involved in trunk NCC emigration. At trunk level, it has been shown that a BMP-Wnt1 signaling cascade controls NCC emigration (Sela-Donenfeld and Kalcheim, 1999; Burstyn-Cohen et al., 2004). The regulation of that cascade is exerted through the caudal (high)-rostral (low) gradient of the BMP inhibitor Noggin, which in turn is controlled by undetermined signals coming from somites (Sela-Donenfeld and Kalcheim, 2000).

In the paraxial mesoderm, the FGF and RA pathways operate as a signaling switch that controls the R-C sequence of mesodermal and neural development. Opposite gradients of declining caudal FGF and rostral RA signaling in the extending body axis create a wavefront, which determines the onset of neuronal differentiation and patterning in newly generated spinal cord (Diez del Corral et al., 2002, 2003) and also positions somite boundaries (Dubrulle et al., 2001; Diez del Corral et al., 2003). The trunk neural tube is generated during a long period of time as the main body axis extends caudally, and trunk neural crest is also generated after this R-C sequence. Thus, FGF and RA signaling pathways are candidates to coordinate NCC development with somite and neuron formation as the embryo elongates.

In this work, using both gain- and loss-of-function approaches, we establish that FGF signaling through the MAPK pathway prevents the initiation of trunk NCC specification and, consequently, NCC EMT. In contrast, RA signaling triggers the EMT of specified NCCs. Furthermore, we show that FGF and RA signaling control the timing of EMT and emigration in part through modulation of elements of the BMP and Wnt signaling pathways. Thus, opposition of FGF and RA signaling orchestrates the onset of trunk NCC specification and emigration, coordinating them with somite formation and neurogenesis in the extending vertebrate body axis.

Results

Onset of NCC marker expression coincides with FGF8 decline

To investigate whether the paraxial mesoderm has a general influence on NCC specification and migration in the spinal cord, we compared the expression patterns of a cohort of genes involved in dorsal patterning and NCC specification with respect to the formation of somites in chicken embryos at Hamburger and Hamilton (HH) stages 10–14 (Fig. 1, A–G). At the HH10 stage, the caudal open neural plate expressed dorsal patterning genes such as *Pax7* (Fig. 1 A; Kawakami et al., 1997), *Pax3* (not depicted; Goulding et al., 1991), *RhoB* (not depicted; Liu and Jessell, 1998), and *Msx1* (not depicted; Liem et al., 1995). This expression is maintained along the neural tube as the body axis extends (Fig. 1 A). More rostrally, when the neural folds move toward the midline to fuse, the expression of the NCC marker *Snail2* (Nieto et al., 1994) was found in the dorsal neural folds (Fig. 1 B) adjacent to the mid-PSM level. Subsequently, expression of *Sox* family genes involved in NCC formation could be observed in the dorsal neural tube. First, *Sox9* (Fig. 1 C; Cheung and Briscoe, 2003) appeared rostral to the initiation of *Snail2* and then *Sox5* (Fig. 1 D; Perez-Alcala et al., 2004). Finally, adjacent to forming somites, *Sox10* (Fig. 1 E; Paratore et al., 2001) was observed in premigratory NCCs about to emigrate.

This order in the expression of the genes described is maintained throughout stages HH12–14 (unpublished data). However, at HH10, *FoxD3*, an NCC specifier (Stewart et al., 2006), was not expressed dorsally in the neural folds (Fig. 1 F). Only by HH12 could *FoxD3* mRNA be observed at the rostral PSM level (Fig. 1 G).

The initiation of the expression of NCC markers seems to coincide with the transition zone where neural progenitors stop expressing caudal neural markers and initiate ventral patterning gene expression. This transition is governed by the opposing activities of the FGF and RA signaling gradients (Diez del Corral et al., 2003). In fact, by in situ hybridization of half embryos, we showed that the onset of *Snail2* expression coincided with the decline of the caudal neural gene *Sax1* expression (Fig. 1 H; Bertrand et al., 2000) and the appearance of the ventral patterning gene *Pax6* (Fig. 1 I; Bertrand et al., 2000). Moreover, the initiation of *Snail2* expression is close to the decay of *FGF8* transcripts in the neural tube (Fig. 1 K), and high levels of *Snail2* mRNA coincided with the onset of the RA-synthesizing enzyme *Raldh2* expression in the adjacent mesoderm (Fig. 1 J).

In summary, NCC markers are progressively transcribed in a precise temporal–spatial order in the presumptive region of premigratory NCCs. Moreover, these data suggest that the onset of specification and EMT of NCCs could be controlled by FGF and RA signaling gradients (Fig. 1 L).

FGF signaling controls the onset of trunk NCC specification through the MAPK pathway

FGF signaling is involved in the maintenance of the neural caudal stem zone, and it also represses neuronal differentiation and ventral patterning (Bertrand et al., 2000; Diez del Corral et al., 2003). To determine whether the onset of NCC specification was regulated by the decline of the caudal gradient of FGF8 signaling, we used the FGF receptor (FGFR) type 1 (FGFR1) antagonist SU5402 (Mohammadi et al., 1997). Cultured HH11 embryos exposed to this drug for 4 h exhibited a severe downregulation of the well-known FGF signaling target *Sprouty2*

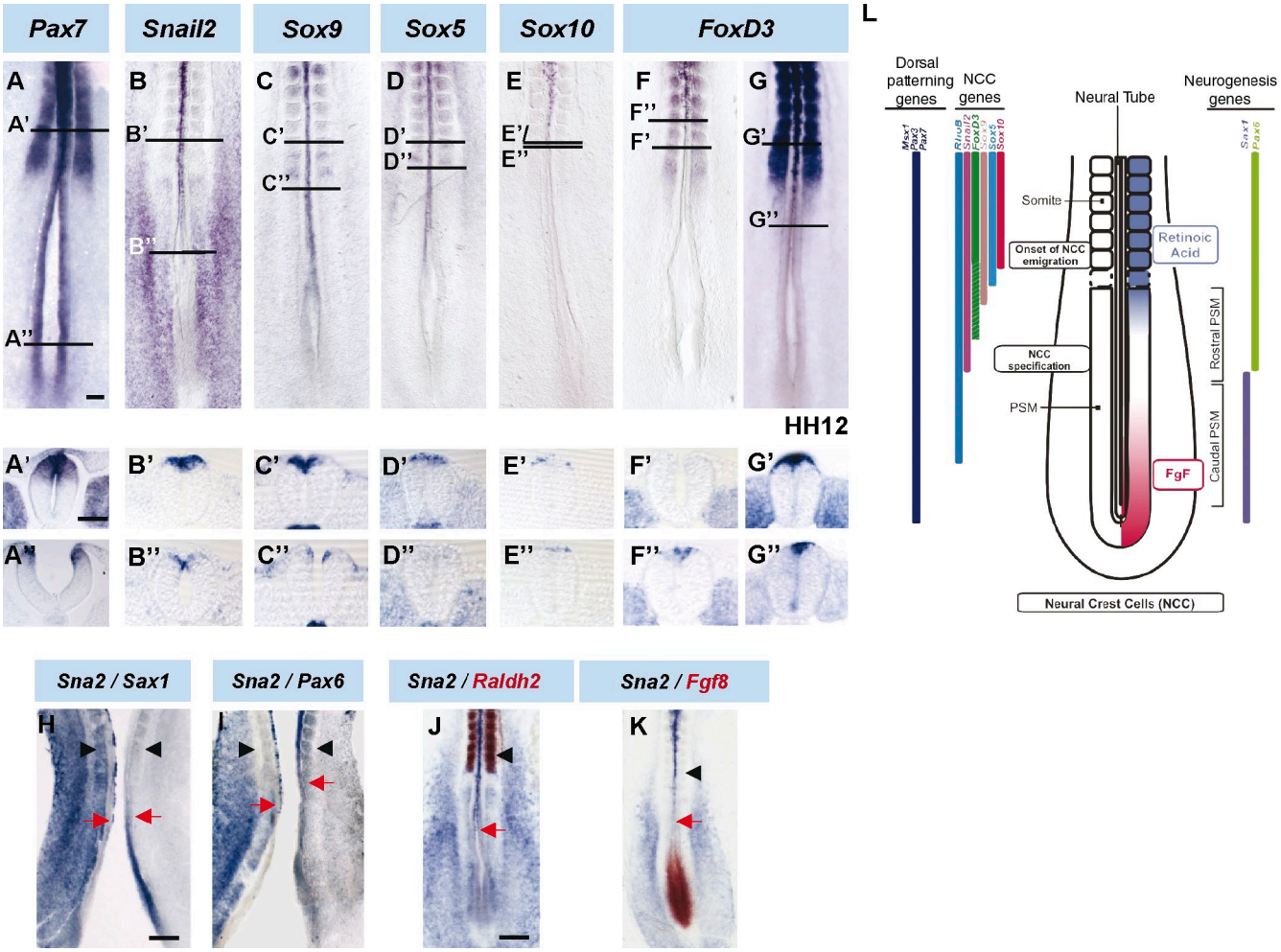

Figure 1. **The onset of expression of NCC markers along the R-C axis coincides with FGF8 decline.** (A–K) Gene expression analysis of stages HH10 (A–F and H–K) and 12 (G) chicken embryos. Transverse sections at the last formed somite level (A′–G′) or at the onset of gene expression in the dorsal neural tube (A′′–G′′; indicated by horizontal lines in the corresponding figures). (H and I) *Snail2* (H and I, left), *Sax1* (H, right), or *Pax6* (I, right) expression in bilaterally dissected embryos. (J and K) Double in situ hybridization for *Snail2* (purple), *Raldh2* (J, red), and *FGF8* (K, red). Black arrowheads point to the last formed somite, and red arrows point to the border of gene expression. (L) Schema of the approximate axial level of different gene expression in relation to NCC development. Bars: (A, for A–G) 100 µm; (A′, for A′–G′ and A′′–G′′) 50 µm; (H, for H and I) 200 µm; (J, for J and K) 300 µm.

(n = 13/13; Fig. 2 B; Minowada et al., 1999) in comparison with control DMSO-treated embryos (n = 0/12; Fig. 2 A). After a 4-h culture with SU5402, *Snail2* expression was enhanced in the dorsal part of the neural tube and was prematurely initiated at the level of Hensen's node (n = 11/12; Fig. 2 F) in comparison with control embryos (n = 4/18; Fig. 2 E). A similar premature *Snail2* up-regulation was observed using the specific FGFR1 inhibitor PD173074 (n = 7/7; Fig. S1; Skaper et al., 2000) and was quantified using quantitative RT-PCR as a twofold increase in relative *Snail2* mRNA levels in PD173074 with respect to DMSO-treated samples in the neural tube at the level of the caudal PSM (2.06 [1.77–2.39]; Fig. S1). As a control, a similar quantitative RT-PCR analysis showed a threefold decrease in *Sprouty* relative mRNA levels in PD173074 with respect to DMSO-treated samples (0.31 ± 0.16; Fig. S1). PD173074 and SU5402 not only inhibit FGFR signaling but also target VEGF receptors (VEGFRs; Mohammadi et al., 1997, 1998). To determine whether these effects are specifically mediated by FGFR signaling, we used a specific VEGFR inhibitor, KRN633 (Nakamura et al., 2004). This did not alter the onset of *Snail2* expression (n = 12/15; Fig. S2) in relation to control DMSO-treated embryos (n = 13/15; Fig. S2). However, FGFR1 inhibition either with PD173074 or SU5402 did not alter the expression of *FoxD3*, another NCC specifier (n = 4 and 7, respectively; Fig. S1 and not depicted), with respect to control embryos (n = 9). Together, these results indicate that FGF caudal gradient prevents the premature expression of the early NCC specifier *Snail2* in the caudal neural tube.

Activation of the tyrosine kinase FGFR can initiate transduction via several downstream pathways including MAPK and phosphatidylinositol 3-kinase (PI3K; Schönwasser et al., 1998). Both pathways have been involved in the transmission of FGF signaling during early stages of neural development (Ribisi et al., 2000; Stavridis et al., 2007), and dual phosphorylated MAPK has been specifically detected in the caudal FGF signaling domain (Lunn et al., 2007). We investigated the potential role of the MAPK kinase (MEK)–extracellular signal-regulated kinase (ERK) regulatory pathway in the control of NCC

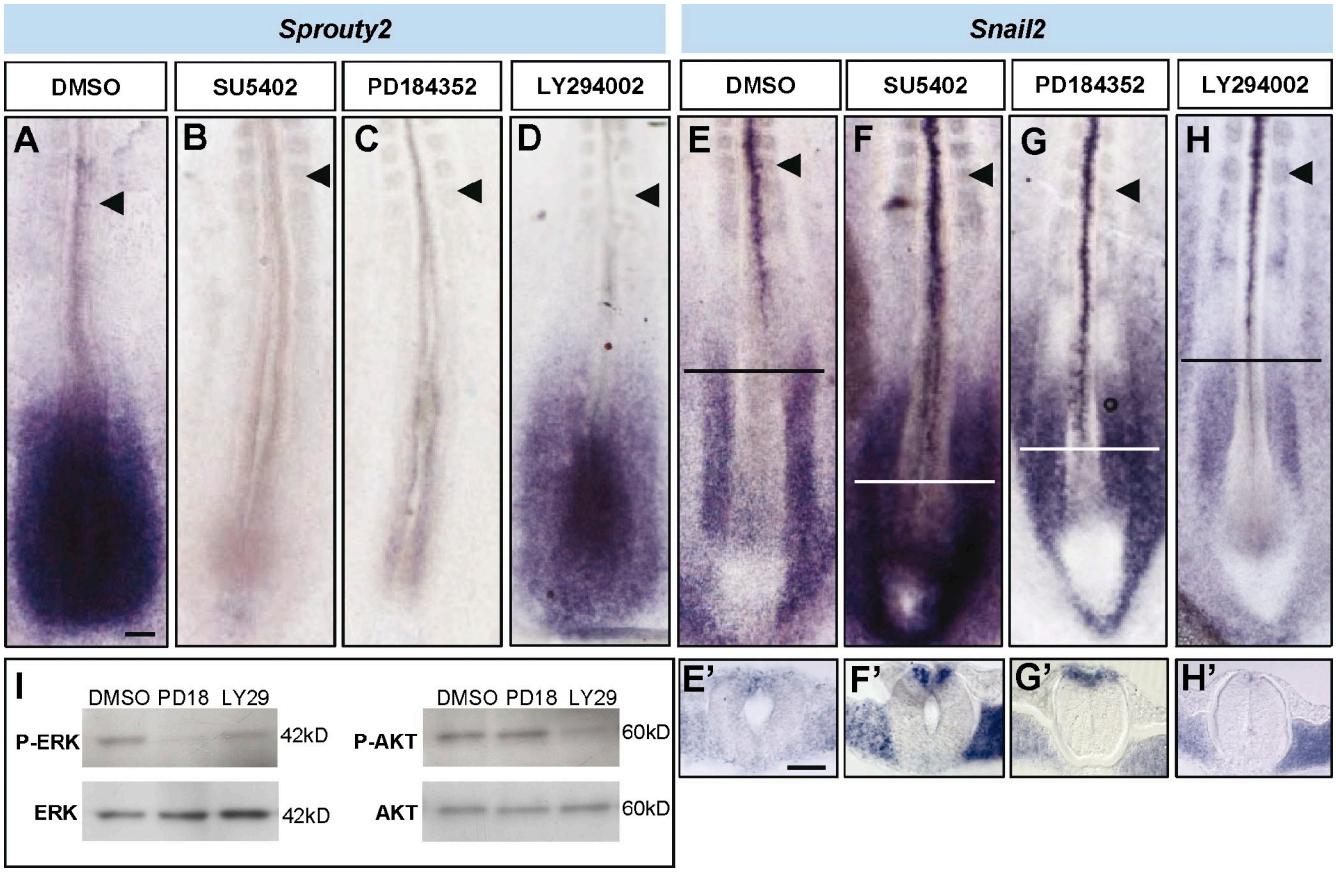

Figure 2. **FGF signaling controls the onset of trunk NCC specification through the MAPK pathway.** (A–H) Stage HH11 and 12 embryos cultured for 4 h in the presence of control (DMSO) or inhibitors for FGFR1 (SU5402), MEK (PD184352), or PI3K (LY294002) and analyzed for *Sprouty2* expression (A–D) and for *Snail2* (E–H). Black arrowheads point to the last formed somite. (E′–H′) Transverse sections at the level are indicated by horizontal lines in the corresponding figures. (I) Western blot analysis from embryos treated with DMSO or the different inhibitors to detect levels of phosphorylated ERK (p-ERK) in comparison with total ERK and levels of phosphorylated AKT (p-AKT) in comparison with total AKT. Results shown are representative of at least three experiments. Bars: (A, for A–H) 100 µm; (E′, for E′–H′) 50 µm.

specification by selectively suppressing activation of MEK1 with the drug PD184352. In HH11 and 12 embryos cultured for 4 h, this drug effectively down-regulated the expression of a direct target of FGF signaling, *Sprouty2* (n = 7/7; Fig. 2 C), and reduced ERK1/2 phosphorylation (92% decreased in phospho-ERK/relative to total ERK; n = 3; Fig. 2 I) in comparison with DMSO-treated embryos (n = 6; Fig. 2, A and I). As with inhibition of FGFR1, blockage of the MAPK pathway leads to a premature and enhanced caudal expression of the NCC specifier *Snail2* (n = 4/4; Fig. 2 G). On the other hand, blockage of the PI3K pathway using the LY294002 treatment, which effectively reduces AKT phosphorylation (73% decreased in phospho-AKT/relative to total AKT; n = 3; Fig. 2 I), had very little effect on *Sprouty2* (n = 1/7; Fig. 2 D; Echevarria et al., 2005) and on *Snail2* mRNA expression (n = 0/4; Fig. 2 H). In conclusion, FGF signaling acting through the MAPK but not the PI3K pathway is required to prevent premature *Snail2* expression in NCCs and, consequently, to delay NCC specification.

The FGF signaling pathway controls the initiation of trunk NCC emigration

Premature specification of NCCs could lead to premature emigration at axial levels previous to somite formation. In the aforementioned experiments, NCCs from embryos incubated with FGFR1 inhibitors for 4 h that prematurely expressed *Snail2* were not able to emigrate, as assessed by the expression of *Sox10* (n = 9; Fig. S1 and not depicted). To better test the consequence on NCC emigration, we examined the effect of blocking FGF signaling for longer periods of time using a dominant-negative FGFR1-EYFP protein (dn-FGFR1-EYFP; Yang et al., 2002) introduced into the right caudal hemitube at HH10 and 11. 18–20 h after electroporation, this construct effectively blocked the expression of FGF signaling targets such as *Sprouty2* (n = 7/9; Fig. S3; Minowada et al., 1999) and induced *Pax6* expression (n = 5/6; Fig. S3; Bertrand et al., 2000) in the neural tube in comparison with control pCIG embryos (n = 6 and 4/5, respectively; Fig. S3). Remarkably, dorsal neural progenitors expressing the dn-FGFR1-EYFP protein prematurely activated *Snail2* (n = 4/4; not depicted) and *Sox10* expression and exited the neural tube (n = 9/10; Fig. 3 B, arrowhead) in comparison with the control side or with cells electroporated with a control EGFP (n = 7; Fig. 3 A). Moreover, the progressive disruption of the basal lamina, identified by Laminin expression (Martins-Green and Erickson, 1987), was also more advanced in the side where FGF signaling had been blocked (n = 5/7; Fig. 3 F) with respect to the control side or control embryos (n = 7; Fig. 3 C).

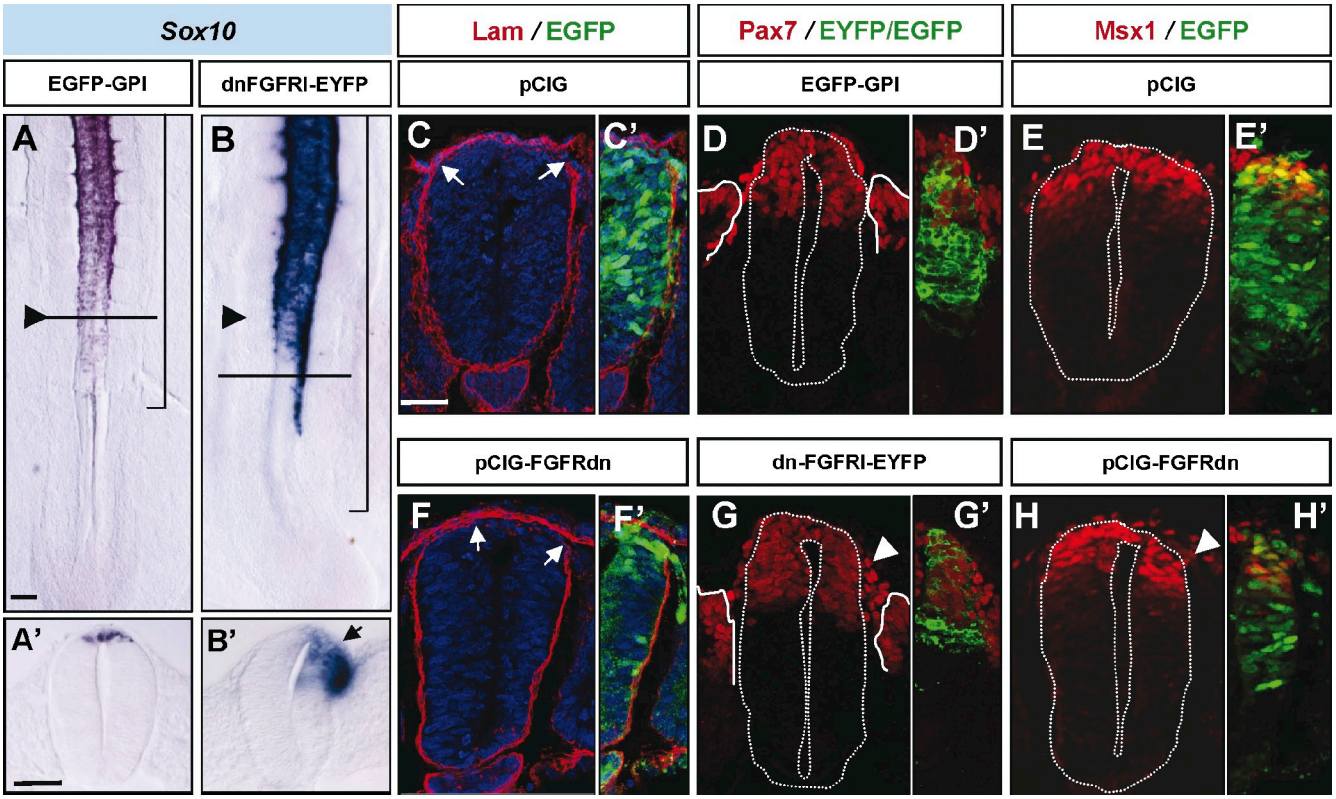

Figure 3. **Blockage of the FGF signaling pathway promotes NCC premature emigration.** (A–H) Stage HH11–13 embryos electroporated on the right neural hemitube with control membrane EGFP (EGFP-GPI), a control nuclear EGFP (pCIG), a dominant-negative truncated version of FGFR1 fused to EYFP (dn-FGFR1-EYFP), or a dn-FGFR in pCIG (FGFRdn-pCIG) construct, as indicated, and analyzed 18–24 h later. (A and B) *Sox10* expression. Black arrowheads point to the last formed somite, and brackets indicate the electroporated area. (A′ and B′) Transverse sections at the level are indicated by horizontal lines in the corresponding figures. The black arrow points to *Sox10* expression in migratory NCCs. (C–H) Immunostaining in electroporated embryos showing in red Laminin (Lam; C and F), Pax7 (D and G), and Msx1 (E and H) expression. (C′–H′) EGFP/EYFP expression in the electroporated hemitube. White arrows point to borders of neural tube basal lamina, and white arrowheads point to an excess of migratory NCCs. The white dotted lines outline the neural tube borders. Bars: (A, for A and B) 50 µm; (A′, for A′ and B′) 40 µm; (C, for C–H) 30 µm.

Migratory NCCs are a mixture of different population subtypes identified by differential gene expression (Del Barrio and Nieto, 2004; Krispin et al., 2010). To determine whether the NCCs delaminating prematurely upon FGF signaling blockage were specifically those expressing *Sox10*, we examined the effects on a whole cohort of NCC markers. After 18–20 h of dn-FGFR1 expression using a nuclear EGFP (pCIG-FGFRdn) as a reporter, there was an increase in the migratory NCC subpopulations expressing Pax7 (n = 10/11; 170 ± 29% with respect to the control side; Figs. 3 G and S4 G), Sox5 (n = 13/13; 159 ± 24% increase; Fig. S4, D and G), AP2 (n = 7/7; 149 ± 13% increase; Fig. S4, E and G), Pax3, *Snail2*, and *FoxD3* (n = 9/9, 4/4, and 5/6, respectively; not depicted) transcription factors in comparison with the control side and with pCIG-electroporated embryos (n = 8, 8, 6, 6, 3, and 8, respectively; Figs. 3 D and S4, A–C).

Remarkably, not all the prematurely migrating NCCs were electroporated GFP$^+$ cells (Fig. S4 D). To determine whether there was a non–cell-autonomous effect upon FGFR blockage, we analyzed the number of Sox5$^+$ migratory cells that were either GFP$^+$ or GFP$^-$ in relation to the number of migratory Sox5$^+$ cells in the control nonelectroporated side (as a way of normalization to reduce axial level variations; Fig. S4 H). The relative number of double GFP$^+$ Sox5$^+$ migratory cells with respect to the total Sox5$^+$ migratory cells in the control side was significantly increased in FGFRdn embryos with respect to control pCIG (68 ± 28% in FGFRdn and 42 ± 15% in pCIG; Fig. S4 H). Interestingly, the relative number of GFP$^-$ Sox5$^+$ cells was also significantly increased in FGFRdn embryos with respect to control pCIG (192 ± 61% in FGFRdn and 65 ± 7% in pCIG; Fig. S4 H). All these data suggest that the premature migration of the FGFRdn-GFP–electroporated cells was also promoting the exit of adjacent non-GFP NCCs, and, thus, the effect on FGFR blockage would be in part non–cell autonomous on NCCs. Moreover, although NCC markers such as *Sox10*, *Snail2*, and Sox5 were prematurely expressed (Fig. 3 B and not depicted) and more ventrally expressed (Sox10; Fig. 3 B′), expression of dorsal markers such as Pax7 and Msx1 was not affected in the neural tube at epithelial somite levels (n = 6 and 10, respectively; Fig. 3, G and H). In conclusion, blocking FGF signaling in the neural tube adjacent to PSM promotes premature NCC specification and emigration from the neural tube.

To determine whether ectopically maintaining the FGF could prevent NCCs from delaminating, we placed FGF8/4-soaked beads in contact with the HH11 and 12 dorsal neural tube at a level in which NCCs have already been specified but before they start *Sox10* expression. As expected, 18 h later, FGF4/8 promoted expression of its direct target *Sprouty2* in the adjacent neuroepithelial cells in HH15–17 embryos (FGF8 n = 3

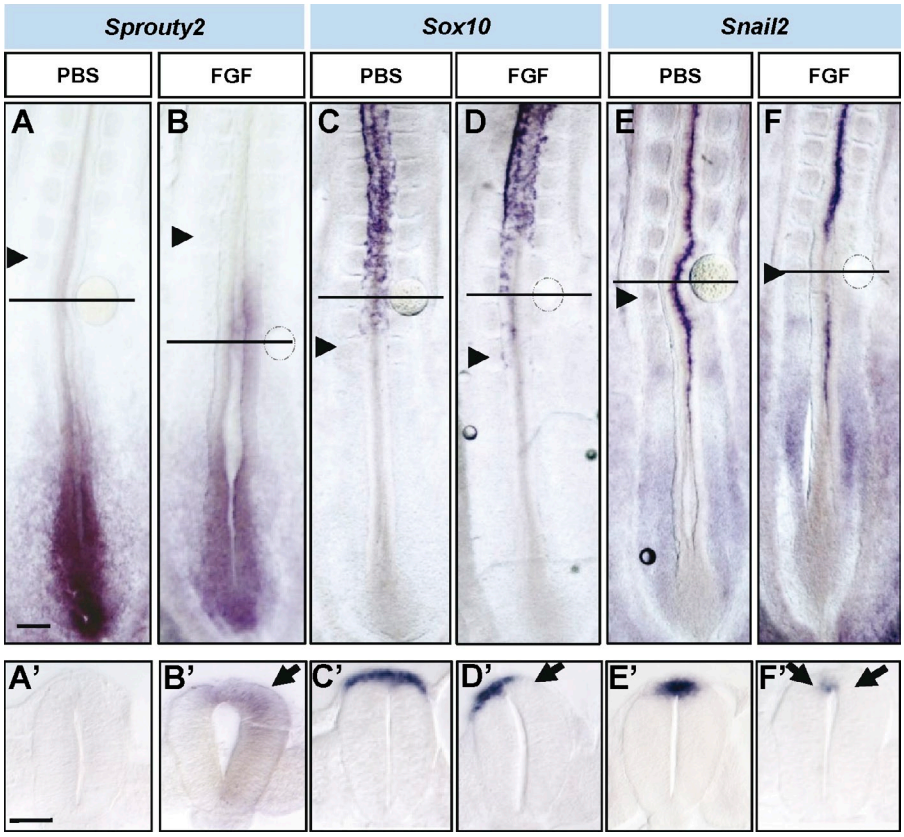

Figure 4. **Ectopic FGF inhibits NCC specification and emigration.** (A–F) Stage HH11 and 12 embryos were exposed to heparin-coated beads either with PBS (A, C, and E) or with FGF4 (B, D, and F) after 16–18 h in culture. In situ hybridization analysis of *Sprouty*, *Sox10*, and *Snail2* expression. Black arrowheads point to the last formed somite. (A′–F′) Transversal sections through the region where the bead was located, indicated by horizontal lines in the corresponding figures. Black arrows point to ectopic expression in B′ and to down-regulation of expression in D′ and F′. Bars: (A, for A–F) 100 µm; (A′, for A′–F′) 40 µm.

and FGF4 $n = 4$; Fig. 4, A and B; Minowada et al., 1999). In contrast to NCCs exposed to control BSA (Fig. 4, C and E, $n = 3$ and 5, respectively), the presence of FGF4/8 drastically reduced *Sox10* (FGF4 $n = 3/4$ and FGF8 $n = 3$; Fig. 4 D) and *Snail2* (FGF4 $n = 4$ and FGF8 $n = 6$; Fig. 4 F) expression and blocked NCC emigration. These data indicate that FGF maintains dorsal neural tube cells uncommitted with respect to neural crest fate and that FGF signaling decrease is necessary to promote NCC specification and subsequent migration from the neural tube.

The timing of NCC emigration confers different migratory behavior

In the trunk region of avian embryos, NCCs migrate in a stereotypical manner, leading to a general ventral to dorsal order of derivative colonization beginning with sympathetic ganglia and, finally, melanocytes (Le Douarin and Kalcheim, 1999). The final localization of crest cells can be predicted from their relative ventrodorsal position within the premigratory domain or by their time of emigration (Henion and Weston, 1997; Krispin et al., 2010). However, it is also possible that distinct properties of the differentiated mesodermal cells that the NCCs encounter during migration influence their trajectories (Harris and Erickson, 2007).

To determine whether the NCCs prematurely forced to delaminate upon blockage of FGF signaling had alterations in their migratory behavior, we followed early NCC migration using wide-field real-time microscopy of trunk dorsal neural tubes in slice culture (Wilcock et al., 2007; Ahlstrom and Erickson, 2009). We used electroporation of H2B-RFP (nucleus)– and EGFP-glycosylphosphatidylinositol (GPI; cell membrane)–expressing vectors into stage HH10 chick embryos to follow individual cells (Fig. 5, A and C). Using MetaMorph software, we first compared the behavior of the migratory NCCs during the initiation or first wave of migration at the level of dissociating somites (somites V–XII) in control EGFP-GPI embryos (Fig. 5 [A, B, and G] and Video 1) in relation to dn-FGFR1-EYFP–electroporated NCCs that started prematurely migrating adjacent to epithelial somites (somites I–IV; Fig. 5 J and Video 3). We observed a similar speed of migration (16.2 ± 1.8 µm/h with respect to 12.4 ± 1 µm/h; Fig. 5 E) and a similar migration straightness (distance covered/length of the trajectory; 0.28 ± 0.07 with respect to 0.15 ± 0.4; Fig. 5 F) of the two spatially different located populations. These results indicate that the prematurely migrating NCCs, upon FGF signaling blockage, at epithelial somite levels have a similar behavior to the first wave of migrating control NCCs facing dissociating somites.

Conversely, we next analyzed the behavior of dn-FGFR1-EYFP–expressing NCCs (Fig. 5 [C, D, and H] and Video 2) that were migrating next to dissociating somites in comparison with the first migrating NCCs expressing EGFP-GPI (Fig. 5 A). The mean speed of the migratory NCCs upon a 12-h period was higher in NCCs expressing dn-FGFR1-EYFP (20.2 ± 1.9 µm/h; Fig. 5 E) with respect to control NCCs (12.4 ± 1 µm/h; Fig. 5, B and E). Moreover, tracking NCC trajectories revealed that most dn-FGFR1–expressing NCCs showed a straight trajectory (Fig. 5 H) contrary to control NCCs that exhibited tortuous trajectories and forward and backward movements (straightness factor of 0.39 ± 0.1 with respect to 0.15 ± 0.03; Fig. 5, F and G).

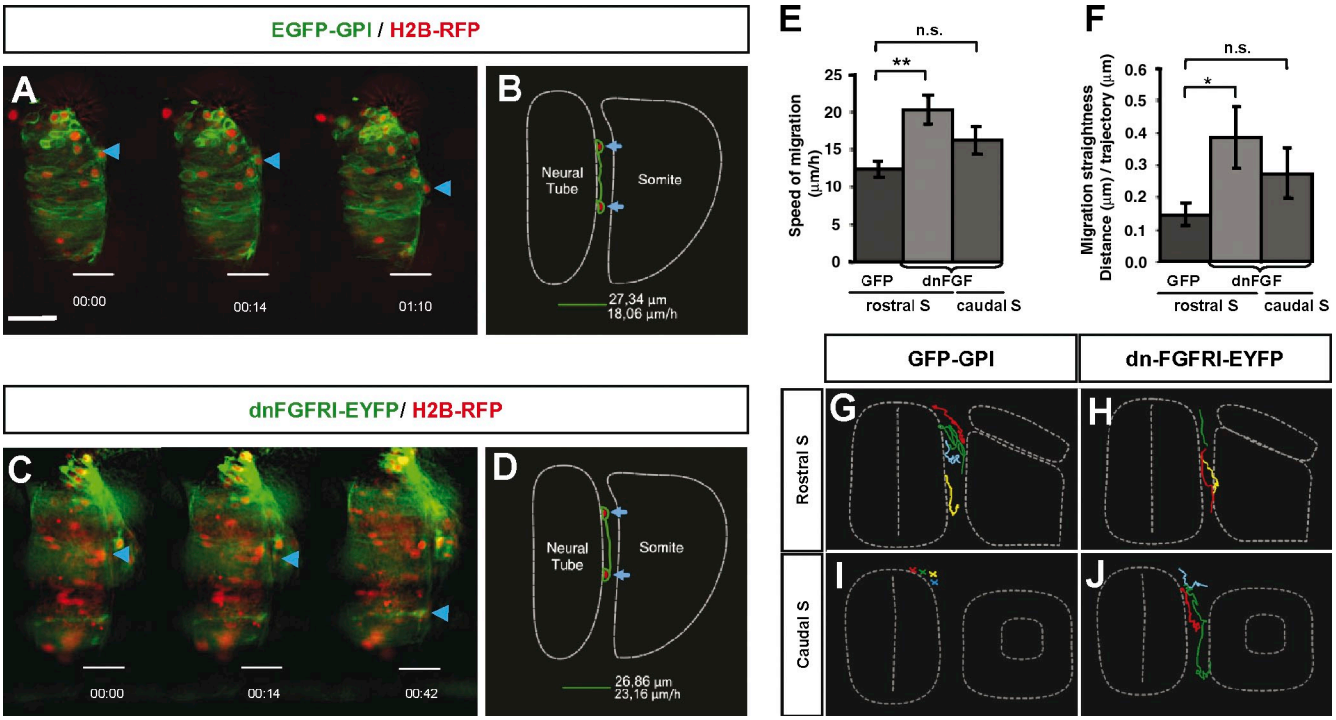

Figure 5. **Analysis of migratory behavior in NCCs after FGF signaling blockage.** (A–D) Chicken embryos at stages HH10 and 11 electroporated on the right neural hemitube with H2B-RFP (red) and with GFP-GPI or dn-FGFR1-EYFP (both green) and analyzed for imaging 14–16 h later. Selected frames taken from a control GFP-GPI (A)– or a dn-FGFR1-EYFP (C)–electroporated embryo at the level of differentiating somites (somite V). Blue arrows and arrowheads point to the same cell along the different frames. The trajectories of cells indicated in A and C are reflected in schemes B and D, respectively. (E and F) Quantitative analysis using MetaMorph software of the speed (E) and straightness (F) of NCC migration analyzed at the level of differentiated or epithelial somites. Error bars indicate the SD of $n = 10$. Statistical significance was examined by Student's *t* test. *, $P < 0.04$; **, $P < 0.003$. n.s., not significant. (G–J) A schematic representation of the trajectories followed by electroporated NCCs either with control EYFP (G and I) or dn-FGFR1-EYFP (H and J) of four representative embryos at the level of epithelial somites (I and J) or differentiating somites (G and H). Bar: (A, for A and C) 20 µm.

This higher speed and straightness of the more advanced delaminating NCCs expressing dn-FGFR1-EYFP could be a property of a more mature late-migrating NCC population in spite of both control and experimental cells facing the same somitic context. In summary, this analysis reveals distinct migratory properties according to the time of exit from the neural tube.

RA signaling is required to control the timing of NCC emigration

It has been shown that somites are required for the control of the onset of NCC emigration (Sela-Donenfeld and Kalcheim, 2000). However, the molecular nature of those signals emanating from the somites remains unknown. RA signaling is highly active in the neural tube at somitic levels, as revealed by in vivo reporter activity driven by RA response elements (RAREs) in mouse embryos (Rossant et al., 1991) and by the expression of a readout of RA signaling, *RAR-β* (the RARE promoter elements of which were used in the RARE-LacZ mouse) in chicken embryos (Olivera-Martinez and Storey, 2007). Moreover, the opposing gradients of FGF and RA pathways operate in concert as a switch that controls progressive neural and limb development (Diez del Corral and Storey, 2004).

To test whether RA could be involved in the control of NCC emigration in concert with FGF signaling, we performed neural tube electroporation of a truncated version of the human α-RA receptor (RAR [RAR-α]) that acts as a dominant-negative form for the three RARs (RARdn–internal ribosome entry site (IRES)–GFP; Novitch et al., 2003). As expected, blocking RAR signaling at HH12 and 13 decreased the expression of Pax6 in neural precursors 24 h after electroporation (Fig. S5; Novitch et al., 2003). In HH12 and 13 embryos in which RA signaling was blocked where NCC emigration was starting, the number of cells expressing *Sox10* was reduced, and there was a dramatic delay in the emigration of *Sox10*$^+$ NCCs ($n = 5/5$; Fig. 6 C) in comparison with the pCIG-electroporated cells ($n = 5/5$; Fig. 6 A). However, more caudally, the initiation of the expression of *Snail2* and *FoxD3*, early markers of NCC specification, was not affected ($n = 5$ and 6, respectively; Figs. 6 F and S5) in comparison with control pCIG-electroporated embryos ($n = 3$ and 8, respectively; Fig. 6 E), indicating that RA is required to establish the onset of NCC emigration independently of NCC specification.

Nevertheless, in HH11–13 embryos electroporated at the level of ongoing NCC migration (somites V–X), RA signaling blockage did not affect the EMT of *Sox10*-expressing NCCs ($n = 4$; Fig. 6 B) compared with the control ($n = 6$; Fig. 6 A). Similarly, blocking RA signaling did not alter the EMT of AP2$^+$ NCCs in comparison with control ($n = 6$; Fig. S5). These data indicate that RA signaling is required to establish the onset but not the maintenance of NCC emigration.

To determine whether RA signaling was not only necessary but sufficient to control NCC emigration, we used a

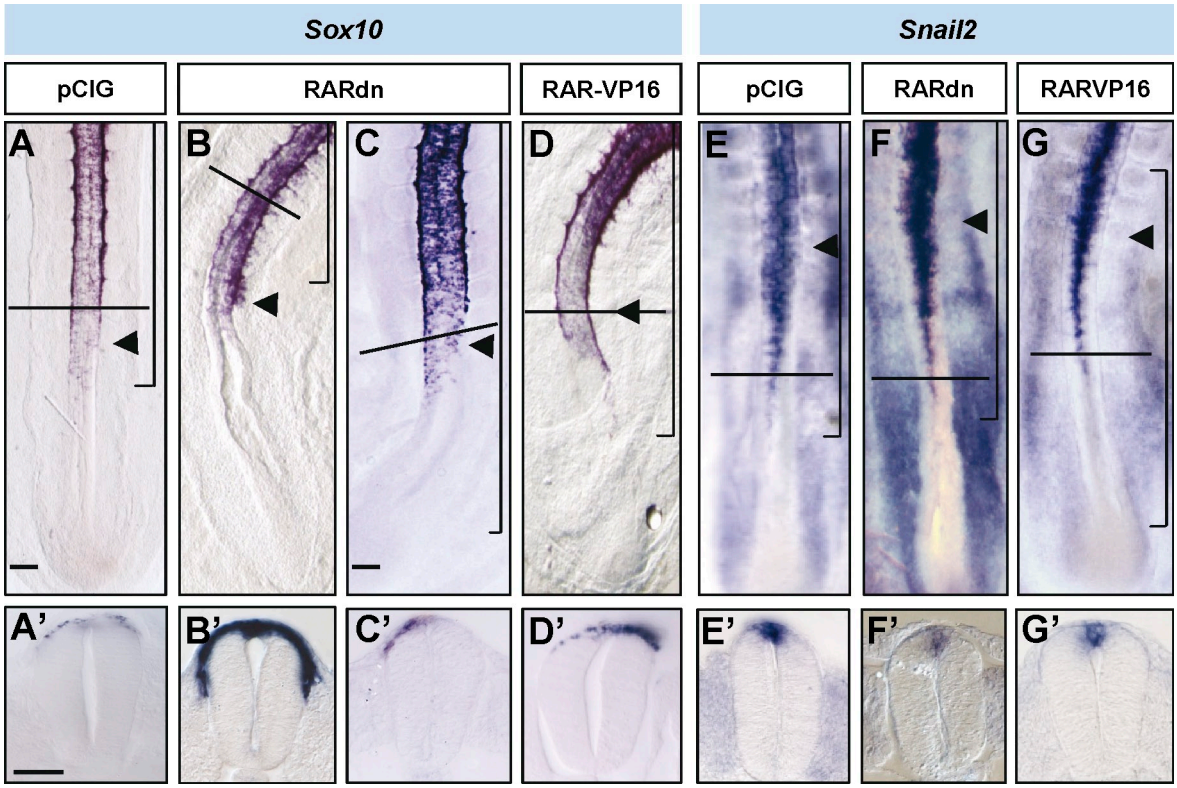

Figure 6. **RA signaling is required at the neural tube to control the timing of NCC emigration.** Chicken embryos at stages HH11–13 electroporated on the right neural hemitube with control pCX-IRES-GFP construct (pCIG), a dominant-negative truncated version of RAR-α (pCIG-RARdn), or a constitutively active form of RAR-α (RAR-VP16) and analyzed 18–24 h later. In situ hybridization of *Sox10* (A–D) and *Snail2* expression (E–G). Black arrowheads point to the last formed somites, and brackets indicate the electroporated area. (A′–G′) Transversal sections at the level are indicated by horizontal lines in the corresponding figures. Bars: (A, for A, B, and D) 100 µm; (C, for C and E–G) 80 µm; (A′, for A′–G′) 45 µm.

constitutively active form of RAR-α fused to the transcriptional activator domain of VP16 (VP16-RAR; Novitch et al., 2003). This construct activates RA target genes in a ligand-independent manner (Castro et al., 1999). VP16-RAR–electroporated neuroepithelial cells at the rostral PSM level delaminated prematurely from the dorsal neural tube in comparison with control embryos, as assessed by *Sox10* expression (n = 5/7; control n = 6; Fig. 6 D). Moreover, the initiation of *Snail2* or *FoxD3* expression in the caudal neural tube was not affected (n = 4 and 7, respectively; control n = 5 and 8, respectively; Figs. 6 G and S5). In summary, RA signaling is both necessary and sufficient to set the right timing for NCC emigration.

Retinoid signaling is required for very early neural crest specification

Our results have shown that RA signaling is not required for NCC specification during neural tube elongation. However, in *Raldh2* mutants, the expression of early NCC markers is severely down-regulated (Ribes et al., 2009). To determine whether that was exclusive of mammalian embryos, we analyzed expression of neural crest markers in vitamin A–deficient (VAD) quails, which represent a retinoid-deficient state (Maden et al., 1996). In normal quails, *Snail2* expression starts in the dorsal neural tube next to mid-PSM (Fig. 7 A), whereas it is strongly reduced in VAD NCCs (Fig. 7 B). Similarly, in RA-deficient conditions, *Sox9* expression is clearly absent from the dorsal neural tube at the rostral PSM level (Fig. 7 D) in comparison with normal embryos (Fig. 7 C). To determine how early RA signaling is required for NCC specification, *Pax7* expression, a key mediator of neural plate border specification (Basch et al., 2006), was examined. In VAD embryos, *Pax7* is absent at the neural plate border (Fig. 7 F) in comparison with normal quails (Fig. 7 E). As the VAD quails represent an early RA-deficient state, these findings suggest that RA signaling is required for the earliest steps in dorsal and NCC specification during gastrulation before the RA activity is restricted to the neural tube adjacent to rostral PSM and is not required for NCC specification during neural tube elongation.

FGF maintains *Noggin* gradient in the caudal neural tube

It has been reported that an R-C gradient of BMP signaling in the dorsal neural tube, generated by the graded expression of the BMP antagonist *Noggin*, is involved in determining the onset of NCC emigration (Sela-Donenfeld and Kalcheim, 1999). As the *Noggin* gradient is controlled by unknown signals coming from the mesoderm (Sela-Donenfeld and Kalcheim, 2000), we tested whether FGF and/or RA could be those signals. First, we determined whether FGF signaling was required for *Noggin* expression, as both coincide in the caudal neural tube (Figs. 1 K and 8 A). In cultured embryos at stages HH10 and 11 briefly exposed (4 h) to the FGFR1 inhibitor PD173074, *Noggin* expression in the neural tube

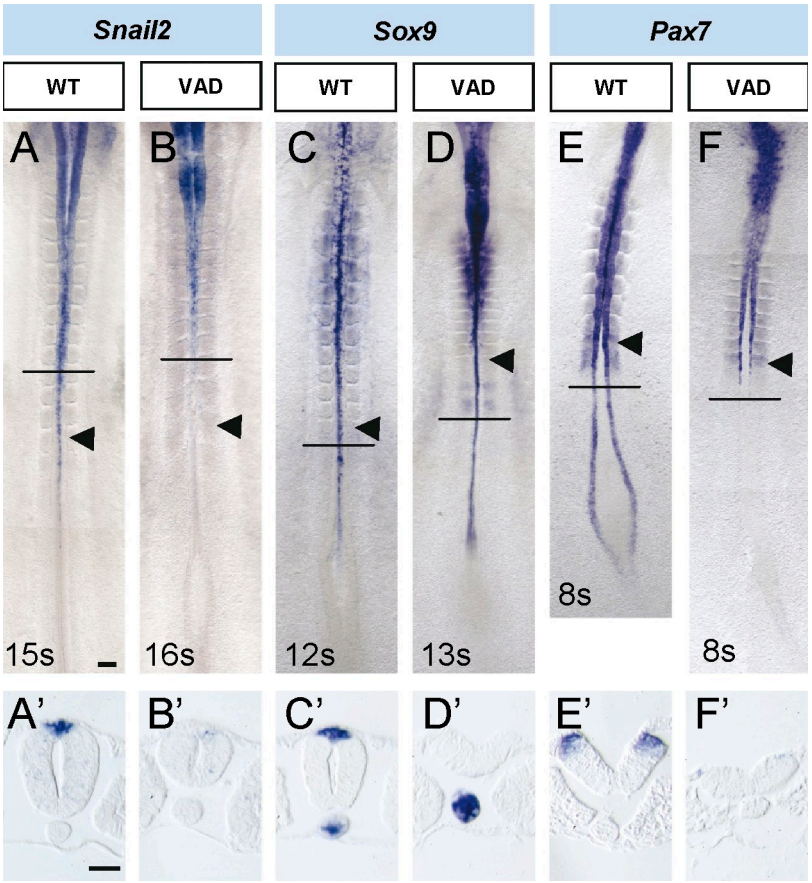

Figure 7. **RA signaling is required for early NCC specification.** (A–F) Comparison of gene expression patterns in the spinal cord in VAD quails and control stage matched quail embryos. (A′–F′) Transverse sections at the level are indicated by horizontal lines in A–F. Black arrowheads point to the last formed somites. Bars: (A, for A–F) 100 µm; (A′, for A′–F′) 50 µm.

was not affected in comparison with control DMSO-treated embryos ($n = 8$ and 8, respectively; Fig. 8, A and B). Similarly, after 18–20 h of dn-FGFR1 electroporation, *Noggin* and *BMP4* expression were not altered in relation to control GFP cells ($n = 7$ and 4, respectively; Fig. 8 [C and D] and not depicted). However, exposing neural tube explants at the rostral PSM level to high doses of FGF4 promoted *Noggin* expression after just 4 h in culture ($n = 10$; Fig. 8 L) relative to BSA control explants ($n = 9$; Fig. 8 K), whereas *Snail2* expression (control $n = 4$; FGF4 $n = 3$; Fig. 8, G and H) was down-regulated, as previously observed with FGF4/8 beads (Fig. 4 F). *Sox10* expression was also down-regulated after 8 h, the time required for *Sox10* mRNA to be detected in control explants (control $n = 12$; FGF4 $n = 9$; Fig. 8, I and J). As a control, *Pax6* was down-regulated by FGF4 in neural tube explants at the somitic level (FGF4 $n = 16$; control $n = 15$; Fig. 8, E and F; Bertrand et al., 2000). Thus, the caudo-rostral FGF signaling gradient is sufficient but not necessary for *Noggin* expression.

To test whether RA was the signal responsible for repression of *Noggin* transcription, RARdn was electroporated in NCCs adjacent to rostral PSM. RARdn-electroporated NCCs exhibited similar levels of *Noggin* expression ($n = 4$; Fig. 8 D) to that of control ($n = 3$; Fig. 8 C). Similarly, in trunk explants at the caudal PSM level exposed for 4 h to the RAR agonist TTNPB, which induced high levels of *Pax6* (TTNPB $n = 10$; control $n = 9$; Fig. 8, M and N; Novitch et al., 2003), *Noggin* expression was similar to that in control DMSO-treated explants 4 and 8 h after culture (control, 4 h, $n = 10$; TTNPB, 4 h, $n = 12$; control, 8 h, $n = 4$; TTNPB, 8 h, $n = 4$; Fig. 8, O and P).

In summary, these results indicate that RA does not control NCC emigration through the down-regulation of *Noggin* gradient. Moreover, FGF signaling is sufficient but not necessary for *Noggin* expression, suggesting that the decrease in FGF signaling is required for *Noggin* down-regulation at somitic levels.

FGF and RA regulate NCC emigration in part through the control of *Wnt1* expression

It has been reported that Wnt ligands are necessary to control *Snail2* expression in NCCs in vivo and are sufficient to induce NCCs by in vitro assays (García-Castro et al., 2002). Moreover, blocking canonical Wnt signaling prevents NCC emigration (Burstyn-Cohen et al., 2004). However, apart from the control by BMP signaling (Burstyn-Cohen et al., 2004), the regulation of the Wnt pathway has not been extensively analyzed in the NCC during axial elongation. We looked to determine whether at NCC emigration FGF and RA signaling could be acting through the modulation of *Wnt1*.

In cultured embryos at stages HH12–14 briefly treated (4 h) with the FGFR1 inhibitor PD173074, the R-C gradient of *Wnt1* expression was prematurely initiated at more caudal levels ($n = 4/7$; Fig. 9 B) in comparison with control DMSO-treated embryos ($n = 10$; Fig. 9 A). Conversely, exposing neural tube explants from rostral PSM levels to FGF4 for 4 h in culture inhibited *Wnt1* expression (FGF4 $n = 6$; BSA $n = 8$; Fig. 9, C and D; described for longer incubation times in Olivera-Martinez

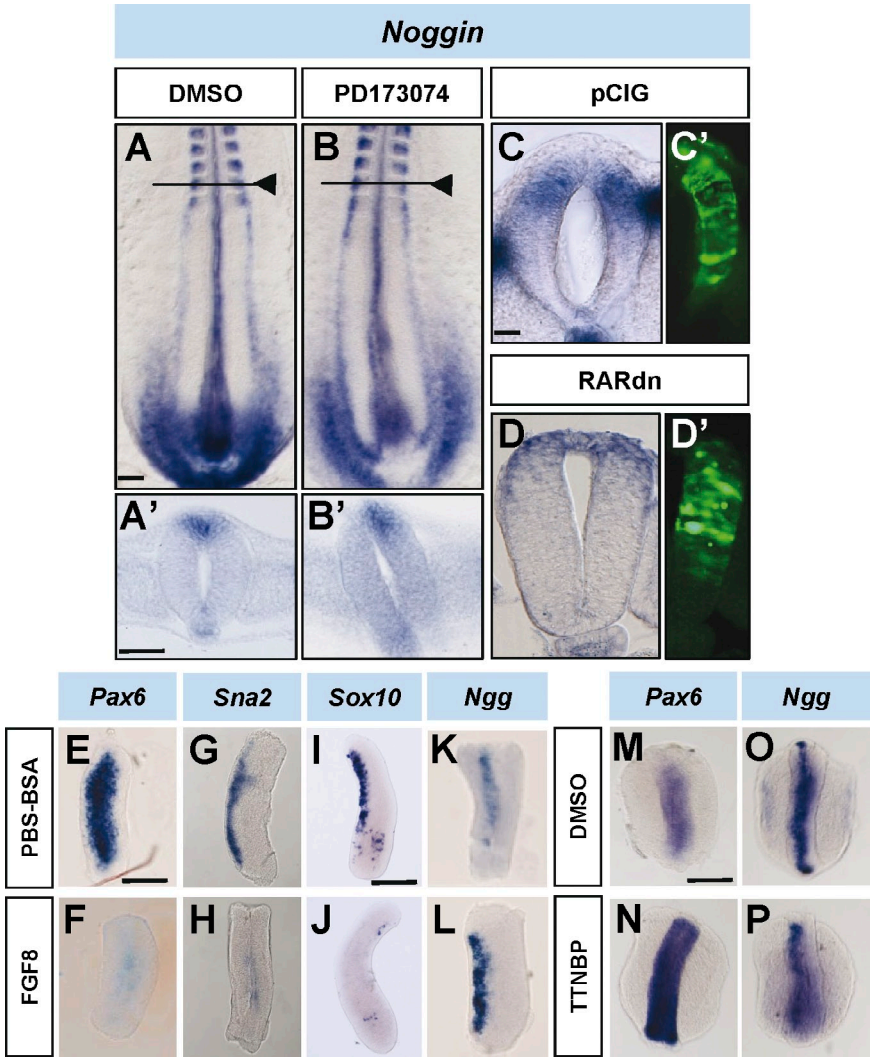

Figure 8. **FGF maintains *Noggin* expression in the caudal neural tube.** (A and B) Stage HH11 and 12 embryos cultured for 4 h in the presence of DMSO (control) or the FGFR1 inhibitor (PD173074) and analyzed for *Noggin* expression. Black arrowheads point to the last formed somites. (A′ and B′) Transversal sections of the respective embryos through the level are indicated by horizontal lines in the corresponding figures. (C and D) Transversal sections of embryos at stages HH11–13 electroporated with control pCIG or with pCIG-dnRAR (RARdn) and analyzed 18–24 h later for *Noggin* expression. (C′ and D′) EGFP in the electroporated area. (E–P) Neural tube explants at the level of rostral PSM (E–H, K, and L) or the entire PSM (I and J) and trunk explants (including neural tube and mesoderm; M–P) at the level of somites (M and N) or caudal PSM (O and P) cultured for 4 or 8 h (only for I and J) in the presence of the indicated medium and analyzed for the expression of the indicated mRNA. Bars: (A, for A and B) 90 µm; (A′, for A′ and B′) 50 µm; (C, for C and D and C′ and D′) 35 µm; (E, for E–H, K, and L) 100 µm; (I, for I and J) 50 µm; (M, for M–P) 85 µm.

and Storey, 2007). In conclusion, FGF signaling levels control the initiation of *Wnt1* expression in the dorsal neural tube.

RA signaling activation in the neural tube adjacent to the somitic level coincides with the initiation of *Wnt1* expression (Figs. 1 K and 9 A). To determine whether RA signaling was required for the control of *Wnt1*, we examined HH10 and 11 VAD quail embryos (Fig. 9, G and H). Strikingly, in VAD embryos, expression of *Wnt1* and *Wnt3a* (Fig. 9, I and J; at older stages in Wilson et al., 2004) was strongly reduced, particularly at the spinal cord level in comparison with normal quail embryos. As this could be caused by the early NCC specification effect described in Fig. 7, we performed trunk explant experiments in chick embryos, where the NCCs have already been specified. Thus, in trunk explants at the rostral half PSM level, *Wnt1* expression was enhanced and caudally expanded after 4 h of exposure to the RAR agonist TTNPB in comparison with DMSO-treated explants ($n = 4$ and 4, respectively; Fig. 9, E and F). However, this effect on *Wnt1* expression was not observed in trunk explants at the caudal PSM level exposed to TTNPB for 4 or 8 h in culture (DMSO, 4 h, $n = 6$; TTNPB, 4 h, $n = 6$; DMSO, 8 h, $n = 4$; TTNPB, 8 h, $n = 4$; unpublished data), where NCCs do not express specifiers like *Snail2* at the time of excision.

In summary, FGF signaling prevents the premature expression of *Wnt1*, whereas RA signaling triggers the initiation of *Wnt1* expression in the dorsal neural tube only at levels in which the NCCs are already specified. Given the short time required for its action in culture, FGF and RA could control the timing of NCC emigration through direct changes in *Wnt1* expression.

Discussion

During embryonic development, it is essential to coordinate the formation of adjacent tissues that maintain close functional relationships. In this work, we have established the mechanism that ensures the correct coordination between the formation of the central and peripheral nervous system in the trunk during the extension of the body axis. We have demonstrated that FGF and RA signaling set the correct timing for the crucial step of NCC EMT and emigration, which is necessary for the distribution of peripheral nervous system progenitors along the body axis.

Our work reinforces the idea that dorsal neuroepithelial progenitors in the caudal neural tube are maintained in an uncommitted state as a result of the presence of a strong FGF–MAPK signaling pathway. Therefore, the caudo-rostral gradient of FGF

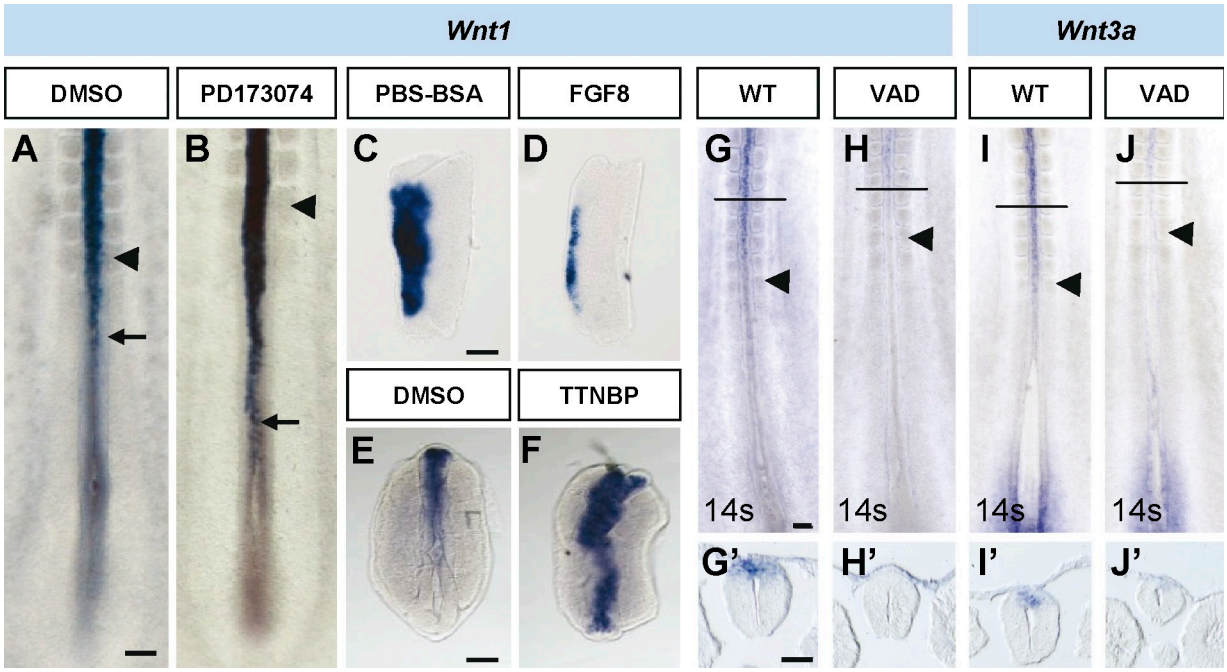

Figure 9. **Onset of *Wnt1* expression is controlled by both FGF and RA signaling.** (A and B) Stage HH11 and 12 embryos cultured for 4 h in the presence of DMSO (control) or FGFR1 inhibitor (PD173074) and analyzed for the expression of *Wnt1*. Arrows point to the onset of expression in the neural tube. (C–F) Explants of neural tube adjacent to rostral PSM (C and D) or whole trunk (including neural tube and mesoderm; E and F) cultured for 4 h in the presence of PBS-BSA (C) or DMSO (E) as a control, FGF8 (D), or the RA agonist TTNPB (F) and analyzed for *Wnt1* expression. (G–J) Comparison of *Wnt1* (G and H) and *Wnt3a* (I and J) expression in VAD quails and control stage matched quail embryos (wild type [WT]). (G′–J′) Transverse sections at the level are indicated by horizontal lines in G–J. Black arrowheads point to the last formed somites. Bars: (A, for A and B) 160 µm; (C, for C and D) 50 µm; (E, for E and F) 42 µm; (G, for G–J) 100 µm; (G′, for G′–J′) 50 µm.

prevents the initiation of the neurogenesis program, the onset of the ventral patterning system (Diez del Corral et al., 2003), and also the onset of trunk NCC specification (Figs. 2, S1, and S2). Thus, in the elongating neural tube, as the dorsal neuroepithelial progenitors are progressively exposed to decreasing FGF signaling levels, they initiate the expression of neural crest specifier genes *Snail2* and *FoxD3*. In our experiments, forcing a reduction in FGF signaling allows neuroepithelial cells to prematurely initiate (just after 4 h) the expression of both the early NCC specifier *Snail2* at caudal levels and, more rostrally, the expression of *Wnt1* (signal required for NCC emigration; García-Castro et al., 2002; Burstyn-Cohen et al., 2004). However, only later on, when those prematurely *Snail2*-expressing NCCs initiate the expression of *FoxD3*, *Sox5*, and finally *Sox10* (after 14 h of FGF signaling blockage; Fig. 3), would they prematurely start EMT from the neural tube at midrostral PSM levels. Essentially, FGF signaling is primarily responsible for the control of the initiation of NCC specification in the trunk, and, as a consequence of that, it controls the timing of EMT and emigration. Furthermore, FGF blockage of NCC emigration is mediated in part by maintaining high levels of *Noggin* and low levels of *Wnt1* in the caudal neural tube (Fig. 10).

Although BMP signaling controls the expression of cytoskeletal components involved in EMT such as *Cadherin6B* (Park and Gumbiner, 2010) and *RhoB* (Liu and Jessell, 1998), altering BMP activity does not change *Snail2* expression and does not affect NCC specification (Sela-Donenfeld and Kalcheim, 1999). Given that most of the NCC specification studies done in *Xenopus* embryos concern the cephalic NCCs (Monsoro-Burq et al., 2003; Hong and Saint-Jeannet, 2007), our work shows that the FGF pathway is, so far, the only signaling pathway clearly controlling the onset of NCC specification at the trunk level. This FGF function could be another example of a general FGF role in controlling the onset of differentiation of all cell types, as they are generated at the tail end.

Our study also points out the relevance of controlling *Snail2* expression to initiate NCC specification. Not only is *Snail2* expression ectopically activated just after 4 h of FGF signaling blockage in comparison with *FoxD3*, which remained unchanged, but *Snail2* is also one of the earliest NCC specifier genes being expressed during trunk NCC formation (Fig. 1; this study) and also during the caudal-most NCC development (caudal vertebrae level) in which *Snail2* expression also precedes that of *Sox9* and *FoxD3* (Osório et al., 2009). The regulation of *Snail* gene expression by FGF seems to be context dependent during development. Although *Snail1* is induced by FGF8 in the lateral mesoderm (Boettger et al., 1999) and primitive streak (Ciruna and Rossant, 2001) and by FGF3 in bone development (de Frutos et al., 2007), it is repressed by FGF in the somites (Boettger et al., 1999), and *Snail2* is repressed in the dorsal neural tube (this study). Furthermore, controlling the right levels of FGF signaling is essential to modulate *Snail* gene expression. In *Xenopus* embryos, FGF signaling is involved in cephalic NCC induction (Monsoro-Burq et al., 2003). However, an excess of FGF signaling inhibits *Snail2* expression and NCC formation (Hong and Saint-Jeannet, 2007).

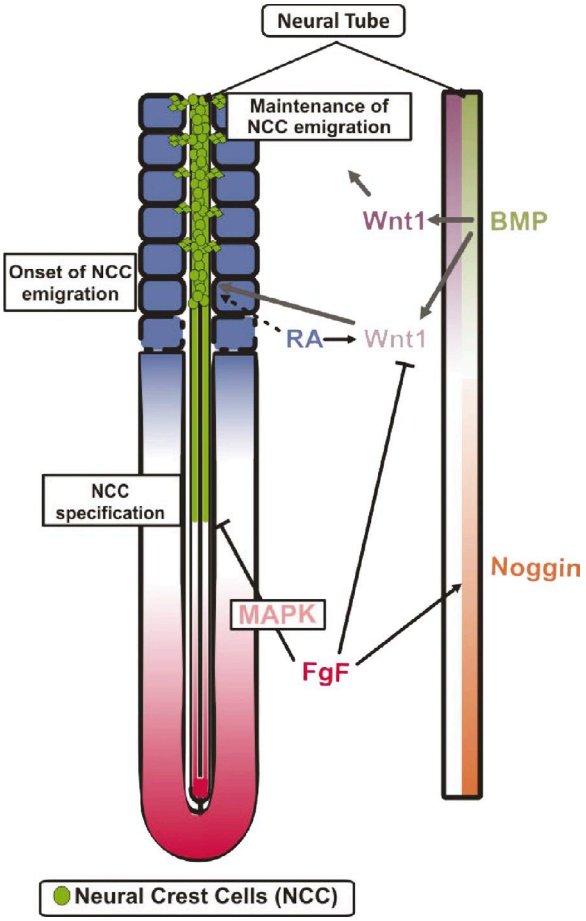

Figure 10. **Signaling pathways involved in the control of NCC specification and emigration during trunk elongation.** The FGF signaling (pink), acting through the MAPK pathway, prevents the onset of NCC (green) specification in the caudal neural tube and, through the regulation of *Wnt1* onset of expression (pale red) and *Noggin* (orange) expression, controls the initiation of NCC emigration. The RA signaling (blue) controls the initiation of NCC emigration by modulating NCC genes (dashed arrow) or by controlling the onset of *Wnt1* expression. The BMP signaling gradient (pale green) promotes the onset and maintenance of NCC emigration through the control of *Wnt1* expression (gray lines; data from Burstyn-Cohen et al., 2004).

In contrast to FGF signaling acting at the caudal level, RA signaling is operating at somitic levels. Our data demonstrate that, at least during trunk elongation, RA signaling is not required for the control of NCC specification but regulates the timing of NCC emigration. Thus, the onset of *Snail2* expression is not affected by changes in RA signaling, but the onset of emigration of *Sox10*$^+$ NCC cells at the midrostral PSM level can be modulated by changing RA signaling.

BMP activity regulates emigration of already specified NCCs (Sela-Donenfeld and Kalcheim, 1999) through the control of *Wnt1* expression (Burstyn-Cohen et al., 2004). RA activity controls emigration modulating, together with FGF signaling, the onset of *Wnt1* expression in the dorsal neural tube at rostral PSM levels (Fig. 10). Thus, our experiments have established that both FGF and RA signaling act as upstream pathways to the BMP/Noggin-Wnt1 signaling cascade to set the right timing for NCC emigration to keep it in register with somite formation. However, the effect of RA on emigration only occurs at rostral PSM and the last-formed somite level. More rostrally, inhibiting RA signaling does not affect ongoing emigration probably because BMP signaling is sufficient to maintain the process (Burstyn-Cohen et al., 2004). Conversely, at most, caudal neural tube level changes in FGF or RA signaling are not sufficient to induce premature *Wnt1* expression (Fig. 9), and, consequently, NCCs cannot delaminate from the most caudal part of the neural tube. This time, the absence of BMP signaling at caudal levels could be responsible for the impossibility of emigration.

The consequences of altering the timing of migration could be crucial for the development of the NCC derivatives. It has recently been shown that the final localization of crest cells can be predicted by their time of emigration (Krispin et al., 2010). Here, we have demonstrated that the different NCC populations do differ in their migratory behavior, as the first migratory cells (including those prematurely forced to migrate in our experiments; Fig. 5) move at lower speed and follow more tortuous paths than later-migrating NCCs. It remains to be seen whether changes in migratory behavior adopted in an inappropriate context (nondifferentiated somites) will have consequences in the final differentiation of the NCCs.

In summary, our data show that there is a limited time window during which the onset of the NCC emigration can be modulated once those cells have acquired the expression of the essential gene network of the NCC specification program. That window coincides with the region where FGF and RA gradients collide, and it is required to keep the emergence of peripheral nervous system progenitors in register with the progressive programs of spinal cord neurogenesis and somite development during trunk axial elongation.

Materials and methods

In situ hybridization

Chicken eggs were incubated at 38°C in an atmosphere of 70% humidity. Embryos were staged according to HH. Embryos were fixed overnight at 4°C with 4% PFA in PBS, rinsed, and processed for whole-mount in situ hybridization. In brief, embryos were treated with 1% H_2O_2 and 10 µg/ml proteinase K, refixed in 4% PFA, and then hybridized overnight at 57°C in 5× SSC buffer containing 50% formamide with digoxigenin- or fluorescein-labeled riboprobes as previously described (Martinez-Morales et al., 2010). The chick *Pax7*, *Snail2*, *Sox5*, *Sox10*, *FoxD3*, *Sox9*, *Sax1*, *Pax6*, *Raldh2*, *FGF8*, *Sprouty2*, *Noggin*, and *Wnt1* riboprobes have been previously described (Cheung and Briscoe, 2003; Diez del Corral et al., 2003; Burstyn-Cohen et al., 2004; Perez-Alcala et al., 2004). Chicken *Pax3* and *Pax7* cDNAs were provided by H. Nakamura (Tokohu University, Sendai, Japan). Chicken *VE-cadherin* was cloned using primers 5′-TCCTTCATTCCTCTCATCCTGTG-3′ (forward) and 5′-TGCCGCTCCAAAACCTTACTTCC-3′ (reverse) following recommendations from C.A. Roselló (Centro Nacional de Investigaciones Cardiovasculares, Madrid, Spain). 4–15 embryos were analyzed for each experimental condition. The probe hybridization was detected with AP coupled with either antidigoxigenin Fab fragments (Roche) or antifluorescein Fab fragment (Roche) and developed with nitro blue tetrazolium chloride/5-bromo-4-chloro-3′-indolyphosphate p-toluidine salt (BCIP) or 2-(4-iodophenyl)-5-(4-nitrophenyl)-3-phenyltetrazolium chloride/BCIP. Hybridized embryos were postfixed in 4% PFA and vibratome sectioned, and immunostaining was performed as described in the Inmunohistochemistry section to visualize GFP$^+$-electroporated cells.

Embryo and explant culture

Chicken embryos at stages HH11 and 12 were cultured onto collagen beds (prepared as a mixture containing 2.9 mg/ml collagen rat tail [BD], 1× L15 [Invitrogen], and 0.6% $NaHCO_3$ to achieve proper polymerization)

covered with Opti-MEM medium (Invitrogen) supplemented with 5% FBS serum, 2 mM glutamine, and 50 µg/ml gentamycin. Inhibitors were added to the culture medium (100 µM SU5402, 100 µM PD184352, 10 µM PD173074, 100 µM LY294002, 10 µM KRN633, or DMSO vehicle). Embryos were cultured for 4 h at 37°C and 5% CO_2 before fixation in 4% (weight/volume) PFA in PBS overnight at 4°C. For FGF treatment, chicken embryos at stages HH10 and 11 were put in early chick culture (Chapman et al., 2001) before being grafted with heparin-coated beads soaked in PBS, FGF8b (50 µg/ml), or FGF4 (50 or 500 µg/ml; an inducer of MAPK-like FGF8; Sigma-Aldrich; Diez del Corral et al., 2002; Casanova et al., 2011). Both FGF4 and FGF8 provoked a decrease in the expression of *Snail2* and *Sox10*, but, obviously, the effect was more extensive with the highest concentration, affecting a larger area of premigratory NCCs (Casanova et al., 2011). After incubation at 38°C for 18–20 h, embryos were either processed for whole-mount in situ hybridization or dissected to obtain explants for quantitative RT-PCR. Retinoid-deficient quail embryos were a gift from E. Gale and M. Maden (Medical Research Council Centre for Developmental Neurobiology, King's College London, London, England, UK), and normal and deficient quail embryos were fixed and processed together for in situ hybridization (Diez del Corral et al., 2003).

Explants were dissected from HH9–13 embryos treated with trypsin to separate the neural tissue from the mesoderm when necessary (Diez del Corral et al., 2002). Explants were cultured in collagen beds and cultured covered in Opti-MEM medium as described above containing either BSA or 360 ng/ml FGF4 (both supplemented with 0.1 ng/µl heparin) or containing 10 µM KRN633 (EMD), 0.1% DMSO, or 10 µM TTNPB (EMD).

Western blot analysis

Western blot analysis was performed by an established method. 20-µg protein samples of each total cell extract were separated by 12% SDS-PAGE, transferred to a polyvinylidene fluoride Immobilon-P membrane (Millipore), and probed with antibodies anti–phospho-AKT (rabbit IgG; Cell Signaling Technology), anti–total AKT1/2 (H136; Santa Cruz Biotechnology, Inc.), anti–phospho-Erk1/2 (Thr202/Tyr204; Cell Signaling Technology), and anti–total Erk1/2 (Invitrogen). Signals were detected with HRP-conjugated secondary antibodies (Jackson ImmunoResearch Laboratories, Inc.) using an ECL Advance Western Blotting Detection kit (GE Healthcare). Quantitative analysis was obtained with a densitometer (GS-800; Bio-Rad Laboratories). Results shown are representative of three or more experiments.

Quantitative real-time PCR

Explants of neural tube together with notochord at caudal PSM levels were dissected from embryos cultured for 4 h in the presence of DMSO or PD173074, and total RNA was isolated using the QuickGene RNA tissue kit SII (Fujifilm). cDNA was synthesized with SuperScript III DNA polymerase (Invitrogen) and random primers (Invitrogen). Real-time PCR was performed in a 7500 PCR System using Power SYBR green Master Mix (Applied Biosystems) and sequence-specific primers (Sigma-Aldrich). Sequences of *Snail2* primers were 5′-AGCCAAACTACAGCGAACTG-3′ (forward) and 5′-TGATAGGGACTGGGTAGCTTTC-3′ (reverse), and sequences for *Sprouty2* primers were 5′-ATCATCTTCAGGGCCAGTTG-3′ (forward) and 5′-TGCTCCCAAGTCTTCTTTGC-3′ (reverse). 18S ribosomal RNA was used as a reference gene. *Sprouty2* levels were determined using the standard curve method, whereas *Snail2* levels were determined by the comparative Ct method following recommendations by Applied Biosystems based on validation experiments assessing whether efficiencies of target and reference are approximately equal. Three lots of 4–12 explants generated in three independent experiments were used. Each of these samples was retrotranscribed, the product was used as a template for each pair of primers in triplicate-well PCR reactions, and the PCR procedure was performed twice.

Constructs

Truncated chick FGFR1c (aa 1–425) fused to EYFP in a Clontech vector (pEYFP-N1) to generate dn-FGFR1-EYFP was provided by C. Weijer (University of Dundee, Dundee, Scotland, UK; Yang et al., 2002) and was also inserted into pCAGGS-IRES–nuclear EGFP (pCIG; Niwa et al., 1991) to generate pCIG-FGFRdn. The pCAGGS vector containing a membrane-tagged EGFP-GPI was used as a control. cDNAs encoding human RAR-α truncation mutant 403 (RAR403; Damm et al., 1993) and a VP16–RAR-α fusion (Castro et al., 1999) cloned into pCIG were provided by B. Novitch (University of California, Los Angeles, CA; Novitch et al., 2003). In this case, pCIG was used as a control vector.

Chick in ovo electroporation

Chick embryos were electroporated with purified plasmid DNA (QIAGEN) at 1–2 µg/µl in PBS with 50 ng/ml Fast green, as previously described (Martinez-Morales et al., 2010). In brief, plasmid DNA was injected in the lumen of HH10 and 12 neural tubes, electrodes were placed on either side of the neural tube, and a train of electric pulses (five pulses at 14 V for 50 ms) was applied using an electroporator (TSS20; Intracel). Eggs were further incubated for 24–48 h and were assayed for EGFP expression in the neural tube. Subsequently, the embryos were fixed and processed for immunohistochemistry or in situ hybridization.

Immunohistochemistry

Embryos were fixed for 2–4 h at 4°C with 4% PFA in PBS, and they were immersed in 30% sucrose solution, embedded in optimal cutting temperature medium, and sectioned on a cryostat (CM1900; Leica). Alternatively, embryos were embedded in 5% agarose/10% sacarose and were sectioned in a vibratome (VT1000S; Leica). For immunohistochemistry, 10-µm cryostat or 40-µm vibratome agarose sections were permeabilized with 0.5% Triton X-100, blocked with 10% FBS, and incubated overnight at 4°C with the primary antibody. After washing, the cryostat sections were incubated for 1 h with secondary antibodies. Primary antibodies against the following proteins were used: Sox5 (Perez-Alcala et al., 2004), GFP (Invitrogen), and Laminin (Sigma-Aldrich). Monoclonal antibodies against Pax7, Msx1 (4G1), Pax6, AP2 (3B5), Pax3, and Snail (62.1E6) were all obtained from the Developmental Studies Hybridoma Bank (developed under the auspices of the National Institute of Child Health and Development and maintained by the University of Iowa). Alexa Fluor 488– and Cy3-conjugated anti–mouse or –rabbit secondary antibodies (Invitrogen) were used for detection, and, after staining, the sections were mounted in Citifluor mounting medium plus bisbenzimide and photographed using a true confocal scanner microscope (SP5; Leica).

Real-time imaging

Embryos at stages HH10 and 11 were electroporated with a concentration of 0.2 µg/µl H2B-RFP either with 1 µg/µl GFP-GPI or dn-FGFR1-EYFP. Embryos were incubated at 38°C for 18 h (for imaging at stages HH15 and 16). Slices of ∼150 µm were taken from the trunk on stage HH16–18 chicken embryos (Wilcock et al., 2007) at the axial level of caudal, epithelial (somite I–IV), or rostral dissociated (somite V–XII) somites. Explants were cultured as described by Wilcock et al. (2007). In brief, slices of ∼150 µm were taken with a microknife, embedded in rat tail collagen type I in coverslip-based Petri dishes (WillCo glass-bottom dish [Intracel] and GWst-3522 coated with poly-L-lysine [Sigma-Aldrich]), and cultured in Neurobasal medium without phenol red (Invitrogen) and supplemented with B-27 to a final 1× concentration with L-glutamine and gentamycin maintained at 37°C with 5% CO_2/air for ∼4 h before imaging. Slices were imaged on a microscope workstation (DeltaVision Core; Applied Precision; Wilcock et al., 2007). The images were taken at least 20 µm past the cut surface of the slice and only where the ectoderm was intact. Images were captured using a 40× 1.30 NA objective lens with a xenon lamp (Applied Precision). Optical sections (exposure time = 50 ms, 512 × 512 pixels; bin = 2 × 2) were spaced by 2 µm and imaged at 7-min intervals for up to 24 h. The images obtained were deconvolved and projected using DeltaVision software (softWoRx; Applied Precision). MetaMorph software (Molecular Devices) was used to analyze the neural crest trajectory and the speed of migration. For each experimental condition, 10 cells were analyzed during a period of 4–12 h from at least four embryos.

Image acquisition and processing

Transmitted light images were acquired in an upright microscope (Eclipse 80i; Nikon) with Digital Sight D5-U1 or DXM1200F cameras using ACT-1 or ACT-2u software (Nikon). Whole embryos and explants were mounted in 50% PBS/50% glycerol and photographed with 10×/0.3 Plan Fluor, 20×/0.75 Plan Apo, or 20×/0.5 Plan Fluor objectives. Vibratome sections were mounted in 50% PBS/50% glycerol and photographed with a 40×/0.75 Plan Fluor objective. Fluorescence-labeled sections were mounted in Citifluor mounting medium plus bisbenzimide, and confocal images were taken using a true confocal scanner system (SP5; Leica) and a 40×/1.40 oil UV-corrected objective. Fluorochromes used were bisbenzimide (Invitrogen), Alexa Fluor 488 (Invitrogen), and Cy3 (Jackson ImmunoResearch Laboratories, Inc.). Images were assembled and corrected in contrast and brightness using Photoshop (CS3; Adobe).

Online supplemental material

Fig. S1 shows an analysis of NCC specification and emigration upon FGFR blockage using the PD173074 inhibitor. Fig. S2 shows that VEGFR activity inhibition does not alter *Snail2* expression in the neural tube. Fig. S3 shows that blockage of the FGF signaling pathway promotes premature *Pax6* expression and prevents *Sprouty2* expression in the neural tube.

Fig. S4 shows that blockage of the FGF signaling pathway promotes premature NCC emigration of several populations. Fig. S5 shows that RA signaling is not required to maintain NCC emigration and does not control the onset of *FoxD3* expression in the neural tube. Video 1 shows the migration of NCCs electroporated with H2B-RFP and with control EGFP-GPI at the level of differentiating somites. Videos 2 and 3 show the migration of NCCs electroporated with H2B-RFP and with dn-FGFR1-EYFP at the level of differentiating (Video 2) and epithelial (Video 3) somites. Online supplemental material is available at http://www.jcb.org/cgi/content/full/jcb.201011077/DC1.

We thank P. Bovolenta for her support and suggestions throughout the project; M.A. Nieto for useful comments on the manuscript; A. Arias, I. Ocaña, and V. Barbero for excellent technical assistance; and E. Cisneros for advice on quantitative RT-PCR. VAD quails were provided by M. Maden and E. Gale.

This work was funded by Ministerio de Ciencia e Innovación grants to A.V. Morales (BFU2005-00762 and BFU2008-02963) and to R. Diez del Corral (BFU2005-02972) and by a Medical Research Council grant to K.G. Storey and I. Olivera-Martínez (G0600234). A.V. Morales was supported by the Ramón y Cajal Program, P.L. Martínez-Morales by a Ministerio de Ciencia e Innovación fellowship, and R.M. Das by a Wellcome Trust grant to K.G. Storey (083611/Z/07/Z).

Submitted: 15 November 2010
Accepted: 5 July 2011

References

Ahlstrom, J.D., and C.A. Erickson. 2009. The neural crest epithelial-mesenchymal transition in 4D: a 'tail' of multiple non-obligatory cellular mechanisms. *Development*. 136:1801–1812. doi:10.1242/dev.034785

Barrallo-Gimeno, A., J. Holzschuh, W. Driever, and E.W. Knapik. 2004. Neural crest survival and differentiation in zebrafish depends on mont blanc/tfap2a gene function. *Development*. 131:1463–1477. doi:10.1242/dev.01033

Basch, M.L., M. Bronner-Fraser, and M.I. García-Castro. 2006. Specification of the neural crest occurs during gastrulation and requires Pax7. *Nature*. 441:218–222. doi:10.1038/nature04684

Bertrand, N., F. Médevielle, and F. Pituello. 2000. FGF signalling controls the timing of Pax6 activation in the neural tube. *Development*. 127:4837–4843.

Boettger, T., L. Wittler, and M. Kessel. 1999. FGF8 functions in the specification of the right body side of the chick. *Curr. Biol.* 9:277–280. doi:10.1016/S0960-9822(99)80119-5

Brewster, R., J. Lee, and A. Ruiz i Altaba. 1998. Gli/Zic factors pattern the neural plate by defining domains of cell differentiation. *Nature*. 393:579–583. doi:10.1038/31242

Bronner-Fraser, M. 1986. Guidance of neural crest migration. Latex beads as probes of surface-substratum interactions. *Dev. Biol. (NY)*. 3:301–337.

Burstyn-Cohen, T., J. Stanleigh, D. Sela-Donenfeld, and C. Kalcheim. 2004. Canonical Wnt activity regulates trunk neural crest delamination linking BMP/noggin signaling with G1/S transition. *Development*. 131:5327–5339. doi:10.1242/dev.01424

Casanova, J.C., V. Uribe, C. Badia-Careaga, G. Giovinazzo, M. Torres, and J.J. Sanz-Ezquerro. 2011. Apical ectodermal ridge morphogenesis in limb development is controlled by Arid3b-mediated regulation of cell movements. *Development*. 138:1195–1205. doi:10.1242/dev.057570

Castro, D.S., M. Arvidsson, M. Bondesson Bolin, and T. Perlmann. 1999. Activity of the Nurr1 carboxyl-terminal domain depends on cell type and integrity of the activation function 2. *J. Biol. Chem.* 274:37483–37490. doi:10.1074/jbc.274.52.37483

Chapman, S.C., J. Collignon, G.C. Schoenwolf, and A. Lumsden. 2001. Improved method for chick whole-embryo culture using a filter paper carrier. *Dev. Dyn.* 220:284–289. doi:10.1002/1097-0177(20010301)220:3<284::AID-DVDY1102>3.0.CO;2-5

Cheung, M., and J. Briscoe. 2003. Neural crest development is regulated by the transcription factor Sox9. *Development*. 130:5681–5693. doi:10.1242/dev.00808

Ciruna, B., and J. Rossant. 2001. FGF signaling regulates mesoderm cell fate specification and morphogenetic movement at the primitive streak. *Dev. Cell*. 1:37–49. doi:10.1016/S1534-5807(01)00017-X

Damm, K., R.A. Heyman, K. Umesono, and R.M. Evans. 1993. Functional inhibition of retinoic acid response by dominant negative retinoic acid receptor mutants. *Proc. Natl. Acad. Sci. USA*. 90:2989–2993. doi:10.1073/pnas.90.7.2989

de Frutos, C.A., S. Vega, M. Manzanares, J.M. Flores, H. Huertas, M.L. Martínez-Frías, and M.A. Nieto. 2007. Snail1 is a transcriptional effector of FGFR3 signaling during chondrogenesis and achondroplasias. *Dev. Cell*. 13:872–883. doi:10.1016/j.devcel.2007.09.016

Del Barrio, M.G., and M.A. Nieto. 2004. Relative expression of Slug, RhoB, and HNK-1 in the cranial neural crest of the early chicken embryo. *Dev. Dyn.* 229:136–139. doi:10.1002/dvdy.10456

Diez del Corral, R., and K.G. Storey. 2004. Opposing FGF and retinoid pathways: a signalling switch that controls differentiation and patterning onset in the extending vertebrate body axis. *Bioessays*. 26:857–869. doi:10.1002/bies.20080

Diez del Corral, R., D.N. Breitkreuz, and K.G. Storey. 2002. Onset of neuronal differentiation is regulated by paraxial mesoderm and requires attenuation of FGF signalling. *Development*. 129:1681–1691.

Diez del Corral, R., I. Olivera-Martinez, A. Goriely, E. Gale, M. Maden, and K. Storey. 2003. Opposing FGF and retinoid pathways control ventral neural pattern, neuronal differentiation, and segmentation during body axis extension. *Neuron*. 40:65–79. doi:10.1016/S0896-6273(03)00565-8

Dottori, M., M.K. Gross, P. Labosky, and M. Goulding. 2001. The winged-helix transcription factor Foxd3 suppresses interneuron differentiation and promotes neural crest cell fate. *Development*. 128:4127–4138.

Dubrulle, J., M.J. McGrew, and O. Pourquié. 2001. FGF signaling controls somite boundary position and regulates segmentation clock control of spatiotemporal Hox gene activation. *Cell*. 106:219–232. doi:10.1016/S0092-8674(01)00437-8

Echevarria, D., S. Martinez, S. Marques, V. Lucas-Teixeira, and J.A. Belo. 2005. Mkp3 is a negative feedback modulator of Fgf8 signaling in the mammalian isthmic organizer. *Dev. Biol.* 277:114–128. doi:10.1016/j.ydbio.2004.09.011

García-Castro, M.I., C. Marcelle, and M. Bronner-Fraser. 2002. Ectodermal Wnt function as a neural crest inducer. *Science*. 297:848–851.

Goulding, M.D., G. Chalepakis, U. Deutsch, J.R. Erselius, and P. Gruss. 1991. Pax-3, a novel murine DNA binding protein expressed during early neurogenesis. *EMBO J.* 10:1135–1147.

Harris, M.L., and C.A. Erickson. 2007. Lineage specification in neural crest cell pathfinding. *Dev. Dyn.* 236:1–19. doi:10.1002/dvdy.20919

Henion, P.D., and J.A. Weston. 1997. Timing and pattern of cell fate restrictions in the neural crest lineage. *Development*. 124:4351–4359.

Hong, C.S., and J.P. Saint-Jeannet. 2007. The activity of Pax3 and Zic1 regulates three distinct cell fates at the neural plate border. *Mol. Biol. Cell*. 18:2192–2202. doi:10.1091/mbc.E06-11-1047

Kawakami, A., M. Kimura-Kawakami, T. Nomura, and H. Fujisawa. 1997. Distributions of PAX6 and PAX7 proteins suggest their involvement in both early and late phases of chick brain development. *Mech. Dev.* 66:119–130. doi:10.1016/S0925-4773(97)00097-X

Khudyakov, J., and M. Bronner-Fraser. 2009. Comprehensive spatiotemporal analysis of early chick neural crest network genes. *Dev. Dyn.* 238:716–723. doi:10.1002/dvdy.21881

Kos, R., M.V. Reedy, R.L. Johnson, and C.A. Erickson. 2001. The winged-helix transcription factor FoxD3 is important for establishing the neural crest lineage and repressing melanogenesis in avian embryos. *Development*. 128:1467–1479.

Krispin, S., E. Nitzan, Y. Kassem, and C. Kalcheim. 2010. Evidence for a dynamic spatiotemporal fate map and early fate restrictions of premigratory avian neural crest. *Development*. 137:585–595. doi:10.1242/dev.041509

Le Douarin, N.M., and C. Kalcheim. 1999. The Neural Crest. Second edition. Cambridge University Press, Cambridge, UK. 445 pp.

Liem, K.F. Jr., G. Tremml, H. Roelink, and T.M. Jessell. 1995. Dorsal differentiation of neural plate cells induced by BMP-mediated signals from epidermal ectoderm. *Cell*. 82:969–979. doi:10.1016/0092-8674(95)90276-7

Liu, J.P., and T.M. Jessell. 1998. A role for rhoB in the delamination of neural crest cells from the dorsal neural tube. *Development*. 125:5055–5067.

Loring, J.F., and C.A. Erickson. 1987. Neural crest cell migratory pathways in the trunk of the chick embryo. *Dev. Biol.* 121:220–236. doi:10.1016/0012-1606(87)90154-0

Lunn, J.S., K.J. Fishwick, P.A. Halley, and K.G. Storey. 2007. A spatial and temporal map of FGF/Erk1/2 activity and response repertoires in the early chick embryo. *Dev. Biol.* 302:536–552. doi:10.1016/j.ydbio.2006.10.014

Maden, M., E. Gale, I. Kostetskii, and M. Zile. 1996. Vitamin A-deficient quail embryos have half a hindbrain and other neural defects. *Curr. Biol.* 6:417–426. doi:10.1016/S0960-9822(02)00509-2

Martinez-Morales, P.L., A.C. Quiroga, J.A. Barbas, and A.V. Morales. 2010. SOX5 controls cell cycle progression in neural progenitors by interfering with the WNT-beta-catenin pathway. *EMBO Rep.* 11:466–472. doi:10.1038/embor.2010.61

Martins-Green, M., and C.A. Erickson. 1987. Basal lamina is not a barrier to neural crest cell emigration: documentation by TEM and by immunofluorescent and immunogold labelling. *Development*. 101:517–533.

Minowada, G., L.A. Jarvis, C.L. Chi, A. Neubüser, X. Sun, N. Hacohen, M.A. Krasnow, and G.R. Martin. 1999. Vertebrate Sprouty genes are induced by FGF signaling and can cause chondrodysplasia when overexpressed. *Development*. 126:4465–4475.

Mohammadi, M., G. McMahon, L. Sun, C. Tang, P. Hirth, B.K. Yeh, S.R. Hubbard, and J. Schlessinger. 1997. Structures of the tyrosine kinase domain of fibroblast growth factor receptor in complex with inhibitors. *Science*. 276:955–960. doi:10.1126/science.276.5314.955

Mohammadi, M., S. Froum, J.M. Hamby, M.C. Schroeder, R.L. Panek, G.H. Lu, A.V. Eliseenkova, D. Green, J. Schlessinger, and S.R. Hubbard. 1998. Crystal structure of an angiogenesis inhibitor bound to the FGF receptor tyrosine kinase domain. *EMBO J.* 17:5896–5904. doi:10.1093/emboj/17.20.5896

Monsoro-Burq, A.H., R.B. Fletcher, and R.M. Harland. 2003. Neural crest induction by paraxial mesoderm in *Xenopus* embryos requires FGF signals. *Development*. 130:3111–3124. doi:10.1242/dev.00531

Morales, A.V., J.A. Barbas, and M.A. Nieto. 2005. How to become neural crest: from segregation to delamination. *Semin. Cell Dev. Biol.* 16:655–662. doi:10.1016/j.semcdb.2005.06.003

Nakamura, K., A. Yamamoto, M. Kamishohara, K. Takahashi, E. Taguchi, T. Miura, K. Kubo, M. Shibuya, and T. Isoe. 2004. KRN633: a selective inhibitor of vascular endothelial growth factor receptor-2 tyrosine kinase that suppresses tumor angiogenesis and growth. *Mol. Cancer Ther.* 3:1639–1649.

Nakata, K., T. Nagai, J. Aruga, and K. Mikoshiba. 1997. *Xenopus* Zic3, a primary regulator both in neural and neural crest development. *Proc. Natl. Acad. Sci. USA*. 94:11980–11985. doi:10.1073/pnas.94.22.11980

Nieto, M.A., M.G. Sargent, D.G. Wilkinson, and J. Cooke. 1994. Control of cell behavior during vertebrate development by Slug, a zinc finger gene. *Science*. 264:835–839. doi:10.1126/science.7513443

Niwa, H., K. Yamamura, and J. Miyazaki. 1991. Efficient selection for high-expression transfectants with a novel eukaryotic vector. *Gene*. 108:193–199. doi:10.1016/0378-1119(91)90434-D

Novitch, B.G., H. Wichterle, T.M. Jessell, and S. Sockanathan. 2003. A requirement for retinoic acid-mediated transcriptional activation in ventral neural patterning and motor neuron specification. *Neuron*. 40:81–95. doi:10.1016/j.neuron.2003.08.006

Olivera-Martinez, I., and K.G. Storey. 2007. Wnt signals provide a timing mechanism for the FGF-retinoid differentiation switch during vertebrate body axis extension. *Development*. 134:2125–2135. doi:10.1242/dev.000216

Osório, L., M.A. Teillet, and M. Catala. 2009. Role of noggin as an upstream signal in the lack of neuronal derivatives found in the avian caudal-most neural crest. *Development*. 136:1717–1726. doi:10.1242/dev.028373

Paratore, C., D.E. Goerich, U. Suter, M. Wegner, and L. Sommer. 2001. Survival and glial fate acquisition of neural crest cells are regulated by an interplay between the transcription factor Sox10 and extrinsic combinatorial signaling. *Development*. 128:3949–3961.

Park, K.S., and B.M. Gumbiner. 2010. Cadherin 6B induces BMP signaling and de-epithelialization during the epithelial mesenchymal transition of the neural crest. *Development*. 137:2691–2701. doi:10.1242/dev.050096

Perez-Alcala, S., M.A. Nieto, and J.A. Barbas. 2004. LSox5 regulates RhoB expression in the neural tube and promotes generation of the neural crest. *Development*. 131:4455–4465. doi:10.1242/dev.01329

Ribes, V., I. Le Roux, M. Rhinn, B. Schuhbaur, and P. Dollé. 2009. Early mouse caudal development relies on crosstalk between retinoic acid, Shh and Fgf signalling pathways. *Development*. 136:665–676. doi:10.1242/dev.016204

Ribisi, S. Jr., F.V. Mariani, E. Aamar, T.M. Lamb, D. Frank, and R.M. Harland. 2000. Ras-mediated FGF signaling is required for the formation of posterior but not anterior neural tissue in *Xenopus laevis*. *Dev. Biol.* 227:183–196. doi:10.1006/dbio.2000.9889

Rickmann, M., J.W. Fawcett, and R.J. Keynes. 1985. The migration of neural crest cells and the growth of motor axons through the rostral half of the chick somite. *J. Embryol. Exp. Morphol.* 90:437–455.

Rossant, J., R. Zirngibl, D. Cado, M. Shago, and V. Giguère. 1991. Expression of a retinoic acid response element-hsplacZ transgene defines specific domains of transcriptional activity during mouse embryogenesis. *Genes Dev.* 5:1333–1344. doi:10.1101/gad.5.8.1333

Saint-Jeannet, J.P., X. He, H.E. Varmus, and I.B. Dawid. 1997. Regulation of dorsal fate in the neuraxis by Wnt-1 and Wnt-3a. *Proc. Natl. Acad. Sci. USA*. 94:13713–13718. doi:10.1073/pnas.94.25.13713

Sauka-Spengler, T., and M. Bronner-Fraser. 2008. A gene regulatory network orchestrates neural crest formation. *Nat. Rev. Mol. Cell Biol.* 9:557–568. doi:10.1038/nrm2428

Schönwasser, D.C., R.M. Marais, C.J. Marshall, and P.J. Parker. 1998. Activation of the mitogen-activated protein kinase/extracellular signal-regulated kinase pathway by conventional, novel, and atypical protein kinase C isotypes. *Mol. Cell. Biol.* 18:790–798.

Sela-Donenfeld, D., and C. Kalcheim. 1999. Regulation of the onset of neural crest migration by coordinated activity of BMP4 and Noggin in the dorsal neural tube. *Development*. 126:4749–4762.

Sela-Donenfeld, D., and C. Kalcheim. 2000. Inhibition of noggin expression in the dorsal neural tube by somitogenesis: a mechanism for coordinating the timing of neural crest emigration. *Development*. 127:4845–4854.

Skaper, S.D., W.J. Kee, L. Facci, G. Macdonald, P. Doherty, and F.S. Walsh. 2000. The FGFR1 inhibitor PD 173074 selectively and potently antagonizes FGF-2 neurotrophic and neurotropic effects. *J. Neurochem.* 75:1520–1527. doi:10.1046/j.1471-4159.2000.0751520.x

Stavridis, M.P., J.S. Lunn, B.J. Collins, and K.G. Storey. 2007. A discrete period of FGF-induced Erk1/2 signalling is required for vertebrate neural specification. *Development*. 134:2889–2894. doi:10.1242/dev.02858

Stewart, R.A., B.L. Arduini, S. Berghmans, R.E. George, J.P. Kanki, P.D. Henion, and A.T. Look. 2006. Zebrafish foxd3 is selectively required for neural crest specification, migration and survival. *Dev. Biol.* 292:174–188. doi:10.1016/j.ydbio.2005.12.035

Teillet, M.A., C. Kalcheim, and N.M. Le Douarin. 1987. Formation of the dorsal root ganglia in the avian embryo: segmental origin and migratory behavior of neural crest progenitor cells. *Dev. Biol.* 120:329–347. doi:10.1016/0012-1606(87)90236-3

Tosney, K.W. 1978. The early migration of neural crest cells in the trunk region of the avian embryo: an electron microscopic study. *Dev. Biol.* 62:317–333. doi:10.1016/0012-1606(78)90219-1

Villanueva, S., A. Glavic, P. Ruiz, and R. Mayor. 2002. Posteriorization by FGF, Wnt, and retinoic acid is required for neural crest induction. *Dev. Biol.* 241:289–301. doi:10.1006/dbio.2001.0485

Wilcock, A.C., J.R. Swedlow, and K.G. Storey. 2007. Mitotic spindle orientation distinguishes stem cell and terminal modes of neuron production in the early spinal cord. *Development*. 134:1943–1954. doi:10.1242/dev.002519

Wilson, L., E. Gale, D. Chambers, and M. Maden. 2004. Retinoic acid and the control of dorsoventral patterning in the avian spinal cord. *Dev. Biol.* 269:433–446. doi:10.1016/j.ydbio.2004.01.034

Yang, X., D. Dormann, A.E. Münsterberg, and C.J. Weijer. 2002. Cell movement patterns during gastrulation in the chick are controlled by positive and negative chemotaxis mediated by FGF4 and FGF8. *Dev. Cell*. 3:425–437. doi:10.1016/S1534-5807(02)00256-3